Effect of inhibition of Loxl2 on inflammasome expression in diabetic nephropathy

Jeon, nara

Department of Medicine

Graduate School

Yonsei University

Effect of inhibition of Loxl2 on inflammasome expression in diabetic nephropathy

Advisor Lim, Beom Jin

A Dissertation Submitted
to the Department of Medicine
and the Committee on Graduate School
of Yonsei University in Partial Fulfillment of the
Requirements for the Degree of
Doctor of Philosophy in Medical Science

Jeon, nara

June 2025

Effect of inhibition of Loxl2 on inflammasome expression in diabetic nephropathy

This Certifies that the Dissertation of Jeon, nara is Approved

Committee Chair	Shin, Jae Il
Committee Member	Lim, Beom Jin
Committee Member	Choi, Hoon Young
Committee Member	Jung, Minsun
Committee Member	Choi, Dae Eun

Department of Medicine
Graduate School
Yonsei University
June 2025

ACKNOWLEDGEMENTS

I wish to express my profound gratitude to all those who contributed to the successful completion of this study. Foremost, I extend my deepest appreciation to Beom Jin Lim and Hoon Young Choi for their invaluable guidance and unwavering support throughout the course of this research. Their expertise and insightful feedback significantly elevated the quality of my work, and their encouragement was pivotal in overcoming the challenges I faced. I am also deeply indebted to Jae Il Shin, Min Sun Jung, and Dae Eun Choi, whose collaboration and stimulating research environment greatly enriched this study. Their meticulous efforts played a crucial role in ensuring the rigor and reliability of the findings presented in this paper.

Finally, I extend my heartfelt thanks to my family, particularly Kwang Soo Shin, for their steadfast support and understanding throughout this research journey. Their encouragement and patience have been an invaluable source of strength and motivation, enabling me to see this project through to its successful completion.

TABLE OF CONTENTS

LIST OF FIGURES

LIST OF TABLES

ABSTRACT

Effect of inhibition of Loxl2 on inflammasome expression in diabetic nephropathy

Diabetic nephropathy (DN) is a leading cause of end-stage renal disease (ESRD) worldwide and represents a major burden in patients with long-standing diabetes. Podocyte injury has emerged as a pivotal early event in the pathogenesis of DN, contributing to proteinuria, glomerulosclerosis, and irreversible loss of renal function. However, the molecular mechanisms driving podocyte dysfunction in diabetic conditions remain incompletely understood.

Lysyl oxidase-like 2 (Loxl2), a copper-dependent amine oxidase, plays an essential role in extracellular matrix (ECM) remodeling by catalyzing the covalent cross-linking of collagen and elastin. Beyond its enzymatic function, Loxl2 has been implicated in various pathological processes, including epithelial-to-mesenchymal transition (EMT), tissue fibrosis, and cancer metastasis. Although Loxl2 has been primarily studied in hepatic, pulmonary, and oncologic contexts, its relevance in renal pathology, particularly in podocyte biology under hyperglycemic conditions, remains largely unexplored.

In the present study, we sought to delineate the functional significance of Loxl2 in diabetic nephropathy, with a particular focus on its expression in podocytes and its interaction with inflammatory signaling pathways. Using a combination of in vitro approaches with CRISPR/Cas9-mediated Loxl2 knockout human podocytes and in vivo experiments employing podocyte-specific Loxl2-deficient mice (Nphs2-Cre; $Loxl2^{flox/flox}$), we demonstrated that Loxl2 expression is significantly upregulated in diabetic kidneys and in cultured podocytes exposed to high glucose and lipopolysaccharide (LPS).

Podocyte-specific deletion of Loxl2 in diabetic mice led to a marked attenuation of glomerular injury, including reduced mesangial expansion, basement membrane thickening, and macrophage

infiltration, accompanied by improved albumin-to-creatinine ratio (ACR). Moreover, mechanistic investigations revealed that Loxl2 deficiency downregulated key components of the Nlrp3 inflammasome pathway, including caspase-1 and interleukin-1β, thereby mitigating the pro-inflammatory milieu within the diabetic glomerulus.

Immunofluorescence analysis further confirmed that Loxl2 was predominantly localized in podocytes and co-expressed with synaptopodin, suggesting its direct involvement in cytoskeletal integrity and filtration barrier maintenance. Importantly, Loxl2 depletion preserved podocyte marker expression under diabetic stress without evidence of compensatory structural damage, indicating a potential protective role of Loxl2 suppression in maintaining podocyte homeostasis.

Together, these findings identify Loxl2 as a previously underrecognized mediator of both structural injury and inflammation in diabetic nephropathy. The dual role of Loxl2 in ECM remodeling and inflammasome activation underscores its therapeutic relevance. Our data suggest that selective inhibition of podocyte-derived Loxl2 may serve as a novel strategy to attenuate the progression of diabetic kidney disease by targeting both fibrotic and inflammatory pathways. Further studies using pharmacologic inhibitors of Loxl2 are warranted to evaluate its translational potential as a disease-modifying target in diabetic nephropathy.

Key words: diabetic nephropathy, kidney disease, Loxl2, podocyte, nlrp3, inflammasome

1. Introduction

Diabetic nephropathy (DN), a leading cause of chronic kidney disease (CKD) and end-stage renal disease (ESRD), is characterized by progressive injury to multiple renal compartments, including glomeruli, tubulointerstitium, and vasculature(1-5). Among these, glomerular damage is often the earliest and most critical event, leading to structural abnormalities such as mesangial expansion, accumulation of extracellular matrix (ECM) components, and glomerular basement membrane (GBM) thickening(4, 6). These alterations eventually culminate in glomerulosclerosis, a hallmark of DN that severely impairs renal filtration function and correlates with increased mortality(5, 7-14). Podocytes, highly specialized epithelial cells lining the outer aspect of the GBM, play a pivotal role in maintaining glomerular filtration integrity(4). They regulate ECM turnover, sustain the architecture of the slit diaphragm, and contribute to the dynamic regulation of GBM permeability. Podocyte injury characterized by detachment, foot process effacement, and apoptosis represents a hallmark of DN and correlates with disease severity(12, 15). Diabetic milieu, including hyperglycemia and oxidative stress, promotes podocyte dysfunction, depletion, and albuminuria, making podocytes central to the progression of DN(16).

The lysyl oxidase (LOX) family, comprising LOX and LOXL1–4 isoforms, is a group of copper-dependent amine oxidases that catalyze the covalent cross-linking of collagen and elastin, thereby stabilizing ECM structure(17, 18). Beyond this classical enzymatic role, LOX family members are implicated in regulating cell proliferation, migration, and differentiation, particularly under pathological conditions such as fibrosis and cancer(19-21). These enzymes have been implicated in processes such as tumor invasion and metastasis, as well as organ development and tissue repair(17, 22). The ability of Lox enzymes to modulate these diverse cellular activities underscores their importance in both physiological and pathological contexts(23). Among them, lysyl oxidase-like 2 (Loxl2) has emerged as a multifunctional enzyme with diverse biological roles in ECM remodeling and disease progression(18, 24). In oncologic settings, Loxl2 is associated with epithelial-to-mesenchymal transition (EMT), tumor invasiveness, and ECM remodeling(19). This cross-linking process is essential for the stabilization and remodeling of ECM, which plays a crucial role in maintaining tissue integrity and function. Loxl2 stands out due to its unique structural and functional characteristics(18). Loxl2 contains a scavenger receptor cysteine-rich (SRCR) domain and a copper-binding site, which are essential for its catalytic activity(20). It functions as an LTQ (lysine tyrosyl quinone)-dependent amine oxidase, enabling it to facilitate the oxidative deamination of lysine

residues in collagen and elastin, leading to the formation of covalent cross-links that stabilize ECM structures(20). The involvement of Loxl2 in ECM cross-linking and remodeling makes it a key player in tissue fibrosis and pathological ECM accumulation. Loxl2 has been studied extensively in the context of cancer, where its overexpression is correlated with poor patient prognosis, particularly in squamous cell carcinoma of the larynx and lungs. It has also been linked to increased metastatic potential in breast and gastric cancers(17, 22, 25). Mechanistically, Loxl2 promotes tumor progression through several pathways. It activates fibroblasts within the tumor microenvironment, leading to the deposition and remodeling of ECM, which provides structural support for tumor growth and invasion. Additionally, Loxl2 induces epithelial-to-mesenchymal transition (EMT) in tumor cells, a process whereby epithelial cells acquire mesenchymal, invasive properties, enhancing their ability to migrate and metastasize. Furthermore, Loxl2 modulates ECM dynamics by regulating tissue inhibitors of metalloproteinases (TIMPs) and matrix metalloproteinases (MMPs), enzymes that play crucial roles in ECM degradation and remodeling(17, 26). Although the role of Loxl2 in cancer biology is well-documented, its involvement in renal pathology is a relatively new area of research. Recent studies have confirmed the expression of Loxl2 in the kidneys of both humans and mice, with a particular focus on its association with the progression of interstitial fibrosis(27-30). Interstitial fibrosis is a common feature of chronic kidney diseases, including diabetic nephropathy, where excessive ECM deposition and structural remodeling lead to impaired renal function(23, 31). In the context of diabetic nephropathy, Loxl2 may contribute to pathological ECM accumulation, promoting fibrosis and ultimately leading to chronic kidney damage. Recent research indicates that Loxl2 expression is not limited to the renal interstitium but is also observed in glomerular structures, including podocytes(27).

Podocytes are essential for maintaining the integrity of the glomerular filtration barrier, and their dysfunction or depletion is a hallmark of diabetic nephropathy(4). The expression of Loxl2 in podocytes suggests that it may directly influence glomerular function, potentially affecting the synthesis and remodeling of the GBM. It has been proposed that Loxl2 may enhance ECM cross-linking within the GBM, contributing to its thickening and the progression of glomerulosclerosis, a critical feature of diabetic nephropathy(23). Additionally, Loxl2 may contribute to the induction of EMT-like changes in renal tubular epithelial cells, promoting fibrosis and altering normal kidney architecture. Given its multifaceted role in fibrosis, inflammation, and ECM remodeling, Loxl2 is emerging as a potential therapeutic target for the treatment of diabetic nephropathy and other chronic

kidney diseases(22, 32). Notably, Loxl2 expression correlates with poor prognosis in several cancers. However, its role in renal disease, particularly in DN, is less well characterized. Recent findings suggest that Loxl2 expression is upregulated in the kidneys during fibrosis and that it may localize specifically to podocytes in diabetic contexts. This podocyte-specific expression implies a potential mechanistic link between Loxl2 and the ECM alterations observed in DN. Simultaneously, inflammation has been recognized as a key driver of DN progression.

The NOD-like receptor family pyrin domain containing 3 (Nlrp3) inflammasome, a cytosolic multiprotein complex, serves as a sensor of metabolic and oxidative stress(33). The Nlrp3 inflammasome is an intracellular multiprotein complex that serves as a crucial mediator in the innate immune response. It becomes activated in response to a variety of stimuli, including high glucose levels, oxidative stress, and advanced glycation end-products (AGEs), all of which are commonly elevated in diabetic environments(34-36). Once activated, the Nlrp3 inflammasome triggers the release of pro-inflammatory cytokines, such as interleukin-1β (IL-1β) and interleukin-18 (IL-18)(5, 33, 37). These cytokines amplify the inflammatory response, leading to the recruitment of immune cells and further exacerbating renal inflammation and fibrosis (5, 38). These cytokines exacerbate renal inflammation, promote immune cell infiltration, and contribute to tubulointerstitial fibrosis and glomerular injury(9, 13). Emerging evidence indicates that Loxl2 and the Nlrp3 inflammasome may functionally intersect. Loxl2 has been implicated in activating fibrogenic signaling pathways that may influence inflammasome priming, while Nlrp3-driven inflammation can modulate ECM turnover and fibrosis. Given this potential interplay, concurrent targeting of Loxl2 and Nlrp3 represents a promising strategy for ameliorating both structural and inflammatory components of DN. Therefore, this study aims to elucidate the role of podocyte-specific Loxl2 expression in the pathogenesis of diabetic nephropathy, with a particular focus on its impact on ECM remodeling and Nlrp3 inflammasome activation. By employing genetic and molecular approaches, we seek to explore whether modulation of Loxl2 can attenuate glomerular injury and inflammation under diabetic stress, thereby identifying novel therapeutic targets for diabetic kidney disease. Inhibition of Loxl2 activity could potentially halt or reverse the fibrotic processes within the kidney, preserving renal function. Inflammation plays a central role in the pathophysiology of diabetic nephropathy, acting as both a driver and consequence of diabetic renal injury. Recent studies have highlighted the central role of Nlrp3 in the pathogenesis of diabetic nephropathy(38, 39). Nlrp3 activation has been associated with podocyte injury, mesangial expansion, and the thickening of the glomerular

basement membrane, all of which are hallmarks of diabetic nephropathy(40, 41). By promoting chronic inflammation and fibrosis, Nlrp3 not only contributes to kidney damage but also accelerates the progression of diabetic nephropathy to ESRD. Consequently, the Nlrp3 inflammasome has emerged as a promising therapeutic target in the treatment of diabetic nephropathy. Research into the mechanisms underlying Nlrp3 activation has revealed potential pathways for therapeutic intervention. For instance, inhibition of Nlrp3 or its downstream signaling molecules has been shown to reduce inflammatory responses and protect renal function in experimental models of diabetic nephropathy. Targeting Nlrp3, therefore, represents a novel strategy for mitigating the progression of diabetic nephropathy, preserving kidney function, and ultimately improving outcomes for patients with diabetes. The interplay between Loxl2 and the Nlrp3 inflammasome suggests that these pathways are not independent but rather interconnected in their contributions to diabetic nephropathy pathology. Targeting Loxl2 has been proposed as a therapeutic strategy to mitigate ECM accumulation and fibrosis, while simultaneously modulating the Nlrp3 inflammasome may help reduce the inflammatory response. Investigating these pathways together offers the potential for synergistic therapeutic interventions aimed at preserving renal function and preventing the progression to diabetic nephropathy.

2. Materials and Methods

2.1 Cell culture

To generate stable Loxl2 knockout human podocytes, the CRISPR/Cas9 gene-editing system was employed with specific single guide RNAs (sgRNAs) designed to target exon 4 of the Loxl2 gene. These sgRNAs were obtained from Dr. Gee's laboratory. HEK 293T cells were utilized as packaging cells and were seeded at a density of 1.5 x 10^6 cells per well in 6-well plates. The cells were then transfected with 0.6 μg of LentiCRISPR v2 (Addgene, Watertown, MA, USA), 0.9 μg of psPAX2 (Addgene, Watertown, MA, USA), and 0.5 μg of pMD2G (Addgene, Watertown, MA, USA) plasmids using the X-tremeGENE HP DNA transfection reagent (Roche, Basel, Switzerland), following the manufacturer's protocol to ensure efficient gene delivery and packaging of lentiviral particles. After 48 hours of transfection, the viral supernatant was collected, filtered through a 0.45 μm filter, and used to transduce human podocytes. Human podocytes were then selected using puromycin (2 μg/ml; Sigma-Aldrich, St. Louis, MO, USA) to enrich for Loxl2 knockout clones. Puromycin-resistant cells were further expanded in RPMI 1640 medium (Thermo Fisher, Waltham, MA, USA) supplemented with 10% fetal bovine serum (FBS; Thermo Fisher, Waltham, MA, USA), 100 U/ml penicillin and streptomycin (Thermo Fisher, Waltham, MA, USA), and 4 μg/ml puromycin to maintain selective pressure. The medium also contained Insulin-Transferrin-Selenium (ITS; Thermo Fisher, Waltham, MA, USA) to support cell growth and proliferation at 33°C, which is considered a permissive condition for podocyte proliferation. To induce differentiation, the podocytes were transferred to RPMI 1640 medium without ITS and incubated at 37°C (non-permissive condition) for at least 14 days. During this period, the cells underwent morphological changes characteristic of differentiated podocytes. The differentiation status was confirmed by assessing the expression of podocyte-specific markers, such as Synaptopodin, using immunofluorescence staining and Western blot analysis. Cells were starved overnight in serum-free medium prior to subsequent experimental treatments to synchronize their metabolic state. Cells were starved overnight in serum-free medium prior to subsequent experimental treatments to synchronize their metabolic state. For the glucose treatment experiment, differentiated podocytes were exposed to high glucose conditions (30 mM D-glucose; Sigma-Aldrich, St. Louis, MO, USA) and lipopolysaccharide (LPS; 1 μg/ml; Sigma-Aldrich, St. Louis, MO, USA) for 6 hours. These conditions were selected to mimic the hyperglycemic and inflammatory environment present in

diabetic nephropathy. Control cells were treated with normal glucose concentration (5.5 mM). The response of the cells, including changes in gene expression and protein levels, was subsequently analyzed to evaluate the impact of high glucose and LPS on Loxl2 knockout podocytes.

2.2 Animals

To investigate the functional role of Loxl2 in podocyte biology and diabetic nephropathy, we generated podocyte-specific Loxl2 conditional knockout (cKO) mice using the Cre-loxP recombination system. The conditional Loxl2 allele was created by flanking exon 4 with loxP sites through CRISPR/Cas9-mediated genome editing (Macrogen, Seoul, Korea). Two guide RNAs (gRNAs) were designed to target intronic regions upstream and downstream of exon 4, and a donor DNA construct was synthesized containing loxP sites along with silent mutations for SnaBI (TACGTA) and ApaLI (GTGCAC) to prevent re-cleavage. The Cas9 protein, guide RNAs, and donor templates were co-injected into C57BL/6 zygotes. Founder (F0) mice were screened by PCR and validated by Sanger sequencing to confirm successful insertion of both loxP sites. Mice harboring the floxed Loxl2 allele ($Loxl2^{flox/flox}$) were then crossed with Nphs2-Cre transgenic mice that express Cre recombinase specifically in podocytes under the control of the Nphs2 (podocin) promoter. Offspring with both the floxed allele and the Nphs2-Cre transgene were identified as podocyte-specific Loxl2 cKO mice (Nphs2-Cre; $Loxl2^{flox/flox}$). Littermates carrying only the floxed allele without Cre expression served as wild-type controls. Genomic DNA was extracted from mouse toe biopsies using the KAPA Express Extract Kit (Roche, Basel, Switzerland) according to the manufacturer's protocol. Mice were genotyped to confirm the presence of the floxed Loxl2 allele and the Nphs2-Cre transgene using polymerase chain reaction (PCR). To detect the floxed Loxl2 allele, PCR was performed using primers listed in **Table 1**, yielding a 223 bp product for the wild-type allele and a 257 bp product for the floxed allele. For identification of the Nphs2-Cre transgene, a separate PCR reaction was conducted with primers also specified in **Table 1**, producing an amplicon of approximately 100 bp. PCR reactions were performed using 2X Taq PCR Master Mix (BIOFACT, Daejeon, Korea), which contains Taq DNA polymerase, dNTPs, $MgCl_2$, and reaction buffer. The amplification protocol consisted of a two-step cycling procedure, beginning with a touchdown PCR to enhance specificity. The first phase included an initial denaturation at 95°C for 2 minutes, followed by 15 cycles of denaturation at 95°C for 15 seconds, annealing starting at 65°C for 30 seconds with a decrement of 1°C per cycle, and extension at 72°C for 1 minute. This was

followed by 30 additional cycles of denaturation at 95°C for 15 seconds, annealing at 55°C for 30 seconds, and extension at 72°C for 1 minute. A final extension was carried out at 72°C for 5 minutes, and reactions were held at 10°C until further analysis. Amplified PCR products were separated on 2% agarose gels stained with ethidium bromide and visualized under ultraviolet light using a GelDoc imaging system (Bio-Rad). All animal procedures were conducted in accordance with the guidelines of the Institutional Animal Care and Use Committee (IACUC) of Yonsei University (Approval No. 2020-0300), following the ARRIVE guidelines. Male mice (8 weeks old) were rendered diabetic by daily intraperitoneal injection of streptozotocin (STZ; 50 mg/kg in citrate buffer, pH 4.5) for 5 consecutive days. Mice with blood glucose >300 mg/dL at day 7 post-injection were classified as diabetic. Mice were fed a high-fat diet (45 kcal% fat; Research Diets, New Brunswick, NJ, USA) for 24 weeks. Blood glucose was monitored every 4 weeks. At the study endpoint, mice were euthanized by CO_2 inhalation followed by cervical dislocation, and kidney tissues were harvested for analysis.

2.3 RNA isolation and real-time PCR

Total RNA was extracted from cultured cells and mouse kidney tissues using the RNeasy Mini Kit (Qiagen, Hilden, Germany) following the manufacturer's protocol, ensuring high RNA purity and integrity suitable for downstream applications. Briefly, cells or tissue samples were homogenized in RLT buffer with β-mercaptoethanol to lyse the samples and deactivate RNases. The homogenized samples were then passed through QIAshredder columns (Qiagen, Hilden, Germany) to ensure complete disruption of cellular components and filtration of debris. Following centrifugation, the lysate was mixed with 70% ethanol and passed through a RNeasy spin column to bind the RNA. The column was washed with RW1 and RPE buffers (Qiagen, Hilden, Germany) to remove impurities, and RNA was eluted with RNase-free water. RNA concentration and purity were measured using a NanoDrop spectrophotometer (Thermo Fisher, Waltham, MA, USA), with A260/A280 and A260/A230 ratios confirmed to be above 1.8, indicating high-quality RNA suitable for reverse transcription. For cDNA synthesis, 1 μg of extracted total RNA was used as a template. The Maxima First Strand cDNA Synthesis Kit (Thermo Fisher, Waltham, MA, USA) was employed according to the manufacturer's instructions. This included a two-step process where the RNA was first combined with a reaction mix containing oligo(dT) and random hexamer primers to ensure comprehensive coverage of mRNA transcripts. The reaction was incubated at 25°C for 10 minutes,

followed by 50°C for 15 minutes for the reverse transcription step, and was then terminated by heating at 85°C for 5 minutes to inactivate the reverse transcriptase. The resulting cDNA was stored at -20°C until further analysis. Quantitative Real-time Polymerase Chain Reaction (qPCR) was conducted using the LightCycler® 96 System (Roche, Basel, Switzerland) to quantify gene expression levels. The PCR reaction mixture included 10 µl of FastStart Essential DNA Probes Master or FastStart Essential DNA Green Master (Roche, Basel, Switzerland), 2 µl of cDNA(20ng), and specific primers and probes listed in **Table 1**. The reaction volume was adjusted to 20 µl with nuclease-free water. For each gene of interest, reactions were run in triplicate to ensure data reliability. The thermal cycling conditions consisted of an initial denaturation step at 95°C for 10 minutes, followed by 40 cycles of 95°C for 15 seconds and 60°C for 1 minute. The fluorescence signal was measured at the end of each cycle to detect the amplification of the target gene. The expression levels of target genes were calculated using the 2^-ΔΔCt method, where ΔCt represents the difference in threshold cycles between the gene of interest and the housekeeping gene, 18S rRNA, which was used as an internal control to normalize gene expression across samples. The ΔΔCt value was derived by comparing the ΔCt of treated samples with that of vehicle-treated control cells or tissues, serving as a baseline. The fold change in gene expression was then calculated and expressed as relative expression levels.

To confirm the specificity of the qPCR amplification, melt curve analysis was performed for each primer set to verify the presence of a single, specific PCR product. All qPCR results were validated by repeating experiments in at least three biological replicates to confirm reproducibility and statistical significance.

2.4 Western blot analysis

Protein extraction from cultured cells and mouse kidney tissues was performed using radioimmunoprecipitation assay (RIPA) buffer (Millipore, Burlington, MA, USA) supplemented with a protease inhibitor cocktail and a phosphatase inhibitor cocktail (Sigma-Aldrich, St. Louis, MO, USA) to preserve protein integrity and prevent dephosphorylation of phosphoproteins. Cell and tissue samples were homogenized in the RIPA buffer on ice to minimize proteolytic activity and then incubated at 4°C for 20 minutes to ensure complete lysis. The lysates were subsequently centrifuged at 14,000 rpm for 20 minutes at 4°C to separate the supernatant containing the soluble proteins from cell debris. The supernatant was collected, and protein concentration was measured

using the bicinchoninic acid (BCA) assay (Pierce, Rockford, IL, USA) according to the manufacturer's instructions, with bovine serum albumin (BSA) as the standard. Absorbance was read at 562 nm using a microplate reader to quantify protein levels accurately. For denaturation, protein samples were mixed with NuPAGE LDS sample buffer (Thermo Fisher, Waltham, MA, USA) containing reducing agent (dithiothreitol, DTT) to disrupt disulfide bonds, ensuring proteins were fully denatured. The samples were heated at 70°C for 10 minutes to complete the denaturation process. Denatured proteins were then separated by sodium dodecyl sulfate-polyacrylamide gel electrophoresis (SDS-PAGE) using a polyacrylamide gel, which provides efficient separation based on molecular weight. Electrophoresis was conducted at 100V for approximately 90 minutes until the protein bands migrated to the appropriate position on the gel. Following electrophoresis, proteins were transferred to a polyvinylidene fluoride (PVDF) membrane (Millipore, Burlington, MA, USA) using a wet transfer system at 100V for 1 hour. The PVDF membranes were pre-activated by soaking them in methanol for a few seconds, then equilibrated in transfer buffer to enhance protein binding efficiency. Post-transfer, the membranes were blocked with 5% skim milk (BD, Franklin Lakes, NJ, USA) in Tris-buffered saline with 0.1% Tween-20 (TBST) for 1 hour at room temperature to prevent nonspecific antibody binding. After blocking, the membranes were incubated overnight at 4°C with primary antibodies specific to the proteins of interest (antibody details are listed in **Table 2**). Primary antibodies were diluted in TBST containing 5% bovine serum albumin (BSA) or 5% skim milk, depending on the antibody's specifications, to maintain antibody activity while reducing background noise. Following primary antibody incubation, the membranes were washed three times with TBST for 10 minutes each to remove unbound antibodies. The membranes were then incubated for 1 hour at room temperature with horseradish peroxidase (HRP)-conjugated secondary antibodies, also diluted in TBST. For protein detection, the membranes were exposed to an enhanced chemiluminescence (ECL) detection reagent (Pierce, Rockford, IL, USA) to visualize the protein bands. The chemiluminescence signal was captured using an Amersham ImageQuant™ 800 system (Cytiva, Amersham, England) to produce high-resolution images of the blots. Exposure times were optimized for each protein to ensure accurate detection while avoiding signal saturation. To quantify the protein bands, images were analyzed using the ImageJ software. Band intensities were measured, and protein expression levels were normalized to those of housekeeping proteins such as β-actin which were run in parallel as loading controls. Densitometric analysis was performed to calculate relative protein expression levels, with values expressed as fold changes compared to

control samples. Experiments were conducted in triplicate to confirm reproducibility and reliability of the results.

2.5 Albumin-to-Creatinine Ratio (ACR)

To evaluate urinary albumin excretion as a marker of kidney function and injury, spot urine samples were collected from mice once a month throughout the experimental period.

Urine collection was performed at a consistent time of day to minimize circadian variations in urinary output. Each sample was collected using metabolic cages for a short period to ensure minimal stress to the animals, and the urine samples were then immediately transferred to sterile microcentrifuge tubes. Samples were stored at −20°C to preserve protein integrity until further analysis. The urinary albumin-to-creatinine ratio (ACR) was measured as an indicator of albuminuria, which is a hallmark of diabetic kidney disease. ACR was determined using the Mouse Albumin ELISA Quantification Set (Ethos Biosciences, Logan Township, NJ, USA) to measure albumin concentrations, and the Creatinine Companion kit (Bioassay Systems, Hayward, CA, USA) for creatinine levels. Both assays were conducted according to the manufacturers' protocols to ensure accuracy and reproducibility. For the ELISA assay, urine samples were thawed and centrifuged briefly to remove any debris before being diluted as required based on expected albumin concentrations. A standard curve was generated using serial dilutions of a mouse albumin standard provided in the kit, allowing for the quantification of albumin levels in the samples. Urine samples and standards were added to the ELISA plate in duplicate, and absorbance was measured at 450 nm using a microplate reader after the addition of the substrate solution and stopping reagent. Albumin concentrations were then interpolated from the standard curve. Simultaneously, creatinine levels in the urine were measured using the Creatinine Companion kit (Bioassay systems, Hayward, CA, USA). Urine samples were processed following the kit's instructions, and creatinine concentrations were determined by measuring the absorbance change at 510 nm after the reaction. The ACR was calculated by dividing the albumin concentration (μg/ml) by the creatinine concentration (mg/dL) for each sample. The ACR values were expressed as micrograms of albumin per milligram of creatinine (μg/mg) to normalize for variations in urine concentration, thus providing a reliable indicator of kidney function over time. The results were analyzed and validated by performing each measurement in triplicate, and experiments were repeated with multiple biological replicates to confirm consistency and accuracy of the data.

2.6 Immunohistochemistry and Immunofluorescence staining

Immunofluorescence staining was performed on paraffin-embedded kidney tissue sections to assess the localization of target proteins. Sections (4 μm thick) were deparaffinized in xylene and rehydrated through a graded ethanol series. Antigen retrieval was carried out by heating the slides in citrate buffer (pH 6.0; Agilent, Santa Clara, CA, USA) using a microwave oven. Endogenous peroxidase activity was blocked with 0.3% hydrogen peroxide for 10 minutes at room temperature. After rinsing with phosphate-buffered saline (PBS), sections were incubated overnight at 4°C with primary antibodies (listed in **Table 2**), followed by fluorophore-conjugated secondary antibodies for 1 hour at room temperature in the dark. Nuclei were counterstained with 4′,6-diamidino-2-phenylindole (DAPI; Sigma-Aldrich, St. Louis, MO, USA) for 5 minutes. Slides were mounted using anti-fade mounting medium (Sigma-Aldrich, St. Louis, MO, USA). Immunohistochemistry was performed on similarly prepared paraffin sections. Following antigen retrieval and peroxidase blocking as described above, sections were incubated overnight at 4°C with primary antibodies against α-smooth muscle actin (α-SMA), F4/80. After washing, sections were treated with horseradish peroxidase (HRP)-conjugated secondary antibodies for 1 hour at room temperature. Visualization was achieved using 3,3′-diaminobenzidine (DAB) as chromogen, and the sections were counterstained with Mayer's hematoxylin, dehydrated, cleared, and coverslipped. For PAS staining, sections were oxidized in 0.5% periodic acid solution (Sigma-Aldrich, St. Louis, MO, USA) for 10 minutes at room temperature to generate aldehyde groups from polysaccharides and mucosubstances. Following a brief wash in distilled water, sections were incubated with Schiff's reagent (Sigma-Aldrich, St. Louis, MO, USA) for 15 minutes in the dark. After another rinse in running tap water for 10 minutes to develop the magenta coloration, sections were counterstained with Mayer's hematoxylin (Dako, Carpinteria, CA, USA) for 1 minute to visualize nuclei. Slides were then washed, dehydrated through ascending ethanol series, cleared in xylene, and coverslipped with Eukitt mounting medium (Sigma-Aldrich, St. Louis, MO, USA). All stained slides, including immunofluorescence, immunohistochemistry, and PAS, were digitally scanned using the Axioscan 7 slide scanner (ZEISS, Oberkochen, Germany), enabling high-resolution whole-slide imaging for both fluorescence and brightfield modalities.

2.7 Statistical analysis

All data are presented as mean ± standard error of the mean (SEM). Statistical comparisons between two groups were performed using unpaired two-tailed Student's t-test (GraphPad Prism version 10, GraphPad Software, San Diego, CA, USA). A p-value < 0.05 was considered statistically significant. In vivo experiments were conducted with 5 mice per group unless otherwise noted. Immunohistochemistry and immunofluorescence images were acquired at 200× magnification, with a scale bar representing 20 μm. All experiments were repeated at least three times to ensure reproducibility.

Table 1. List of the abbreviations

Abbreviation	Definition
ACR	Albumin to creatinine ratio
ACTN4	Alpha actinin 4
AGEs	Advanced glycation end-products
BCA	Bicinchoninic acid
BSA	Bovine serum albumin
CKD	Chronic kidney disease
CRISPR	Clustered regularly interspaced short palindromic repeats
Cas9	CRISPR-associated protein 9
DAB	3,3′-Diaminobenzidine
DAPI	4′,6-Diamidino-2-phenylindole
DKD	Diabetic kidney disease
DMEM	Dulbecco's modified eagle's medium
DN	Diabetic nephropathy
DTT	Dithiothreitol
ECL	Enhanced chemiluminescence
ECM	Extracellular matrix
EMT	Epithelial to mesenchymal transition
ESRD	End stage renal disease
FBS	Fetal bovine serum
GAPDH	Glyceraldehyde 3 phosphate dehydrogenase
GBM	Glomerular basement membrane
gRNAs	Guide RNAs
HFD	High fat Diet
HRP	Horseradish peroxidase
IF	Immunofluorescence
IHC	Immunohistochemistry
IL-1β	Interleukin-1 beta
ITS	Insulin transferrin selenium
KO	Knockout
Loxl2	Lysyl oxidase-like 2
LPS	Lipopolysaccharide
LTQ	Lysine tyrosyl quinone
MMPs	Matrix metalloproteinases
Nlrp3	NOD-like receptor pyrin domain containing 3
PBS	Phosphate buffered saline
PCR	polymerase chain reaction

PVDF	Polyvinylidene difluoride
RIPA	Radioimmunoprecipitation assay
RT	Room temperature
SDS-PAGE	Sodium dodecyl sulfate–polyacrylamide gel electrophoresis
SRCR	scavenger receptor cysteine rich
STZ	Streptozotocin
TBS	Tris buffered Saline
TBST	Tris buffered saline with tween 20
TIMPs	Metalloproteinases
WB	Western blot
WT	Wild type
qPCR	Quantitative real-time polymerase chain reaction
sgRNA	Single guide RNA
α-SMA	Alpha-smooth muscle actin

Table 2. Probes and Primers for Real-Time PCR

Name	Cat.No	Company
Rn18S	Mm03928990_g1	Thermo fisher
Human Loxl2	Hs00158757_m1	Thermo fisher
Mouse Loxl2	Mm00804740_m1	Thermo fisher
	Forward (5'- 3')	**Reverse (5'- 3')**
Human 18S	ACACGGACAGGATTGACAGA	GGACATCTAAGGGCATCACA
Human Nlrp3	ACAATGACAGCATCGGGTGT	AGAAAGATAGCGGGAATGATGA
Human Caspase-1	GCCTGTTCCTGTGATGTGGA	TTCACTTCCTGCCCACAGAC
Human IL-1β	CTGAGCTCGCCAGTGAAATG	TGTCCATGGCCACAACAACT
Mouse Loxl2	CCTTGCCACAGCCAAATAAT	ATGTGGGAAGCCACAGGTAG
Mouse 18S	GCAGGTGTTTGACAACGGCAG	GATGATGGAGTGTGGCACCGA
Mouse Cre	GCGGTCTGGCAGTAAAAACTATC	GTGAAACAGCATTGCTGTCACTT
Mouse Nlrp3	AGCCAGAGTGGAATGACACG	GCAGCTCCAGCTTAAGGG
Mouse Caspase-1	CTTTCTCCGAGGGTTGGAGC	ACCACTCCTTGTTTCTCTCCAC
Mouse IL-1β	GAAGTTGACGGACCCCAAAA	GCCTGCCTGAAGCTCTTGTT

Table 3. Antibodies for Western blot analysis and Immunofluorescence

Primary antibody	**Cat.No**	**Company**	**Dilution**	**Application**
Synaptopodin	ab117702	Abcam	1:1000	Western blot analysis
Synaptopodin	65294	Progen	1:50	Immunofluorescence
Loxl2	AF2639	R&D	1:200	Western blot analysis
Loxl2	bsm-54163R	Bioss	1:50	Immunofluorescence
Loxl2	ab96233	Abcam	1:500	Western blot analysis
Nlrp3	13158	Cell signaling Technology	1:100	Western blot analysis
Nlrp3	ab263899	Abcam	1:500	Western blot analysis
Caspase-1	ab179515	Abcam	1:500	Western blot analysis
IL-1β	12703	Cell signaling Technology	1:100	Western blot analysis
IL-1β	ab234437	Abcam	1:500	Western blot analysis
α-actinin 4	15145	Cell signaling Technology	1:50	Immunofluorescence
F4/80	ab6640	Abcam	1:500	Immunohistochemistry
α-SMA	MAB1420	R&D	1:500 1:1000	Immunohistochemistry Western blot analysis
β-actin	sc-47778	Santacruz	1:5000	Western blot analysis
Secondary antibody	**Cat.No**	**Company**	**Dilution**	**Application**
Anti-rabbit IgG-HRP	7074	Cell signaling Technology	1:5000	Western blot analysis
Donkey anti-goat IgG-HRP	sc-2020	Santacruz	1:5000	Western blot analysis

Goat anti-Mouse IgG -HRP	GTX213111-01	Genetex	1:10000	Western blot analysis
Donkey anti-Mouse IgG (H+L)	A-21202	Thermo Fisher	1:100	Immunofluorescence
Donkey anti-Rabbit IgG (H+L)	ab150076	Abcam	1:100	Immunofluorescence
Rabbit Anti-Rat IgG H&L (HRP)	ab6734	Abcam	1:1000	Immunohistochemistry

3. Results

3.1 Loxl2 knockdown preserves synaptopodin expression in human podocytes under high glucose and inflammatory conditions

To investigate the role of Loxl2 in diabetic conditions, human podocyte cell lines with CRISPR-Cas9-mediated knockdown of Loxl2 were generated(42). The efficiency of the Loxl2 knockdown was validated using Real-time Polymerase Chain Reaction (qPCR) and Western blot analysis, as shown in **Figure 1**. We established four experimental conditions to evaluate the effects of Loxl2 in response to different stimuli: normal glucose concentration (vehicle control), treatment with lipopolysaccharide (LPS, 1 μg/ml), high glucose exposure (30 mM D-glucose), and a combination of LPS and high glucose. In the control human podocytes (plenti v2 cells), both the mRNA and protein levels of Loxl2 were upregulated in response to LPS, high glucose, and the combined LPS + high glucose treatments. In contrast, human podocytes with CRISPR-Cas9-mediated Loxl2 knockdown exhibited a significant reduction in Loxl2 expression under the same conditions. This knockdown was consistent across both the mRNA and protein levels, indicating effective suppression of Loxl2 expression in these experimental groups. Synaptopodin, an actin-associated protein, is critically involved in the maintenance of the podocyte cytoskeleton and the structural integrity of the slit diaphragm(7, 43). This protein plays an essential role in the dynamic regulation of the actin cytoskeleton, which is fundamental to podocyte function and the filtration barrier within the glomerulus(7, 10). In human podocytes, synaptopodin is predominantly localized in the foot processes, where its presence is indicative of podocyte differentiation and functionality. As such, synaptopodin expression is commonly used as a marker for assessing the mature and differentiated state of podocytes, as its expression correlates with the integrity of the podocyte structure. Our results demonstrated that the expression of synaptopodin was significantly decreased in podocytes treated with LPS, high glucose, and LPS combined with high glucose compared to vehicle-treated control cells. Importantly, in podocytes with CRISPR-mediated Loxl2 knockdown, synaptopodin expression was further reduced relative to control cells. This observation suggests a potential regulatory relationship between Loxl2 and synaptopodin, with Loxl2 likely playing a role in the modulation of synaptopodin expression and, consequently, the

maintenance of podocyte structure and function under pathological conditions such as inflammation and hyperglycemia(28). These findings provide novel insights into the role of Loxl2 in podocyte biology, particularly in the context of diabetic nephropathy, where inflammatory and high-glucose conditions are known to disrupt podocyte function and integrity(44, 45). The observed correlation between Loxl2 and synaptopodin expression highlights Loxl2 as a potential therapeutic target for preserving podocyte health and preventing glomerular dysfunction in diabetic conditions.

3.2 Knockdown (KD) of Loxl2 resulted in reduced Nlrp3 inflammasome expression in human podocytes

Nlrp3 is a pivotal component of the inflammasome complex, which plays a crucial role in the innate immune response by regulating the production of pro-inflammatory cytokines(33, 36, 38). In human podocytes, Nlrp3 expression has been implicated in the regulation of inflammatory responses and cellular stress mechanisms. Activation of the Nlrp3 inflammasome in podocytes leads to the secretion of pro-inflammatory cytokines, such as Interleukin-1 beta (IL-1β), which can contribute to podocyte injury and dysfunction. This connection suggests that the dysregulation of Nlrp3 expression in podocytes may play a significant role in the pathogenesis of various glomerular diseases, including diabetic nephropathy. As such, understanding the interplay between Nlrp3 expression and podocyte health could provide critical insights into therapeutic strategies aimed at mitigating podocyte-related kidney damage(36, 41, 46). To investigate whether high glucose exposure induces Nlrp3 inflammasome activation in podocytes, cells were subjected to the following experimental conditions: normal glucose (vehicle control, 5.5 mM), LPS (1 μg/ml), high glucose (30 mM D-glucose, HG), and a combination of LPS and HG. The results demonstrated that treatment with both LPS and high glucose significantly upregulated Nlrp3 and IL-1β mRNA expression, as shown in **Figure 2A**. This upregulation was also observed at the protein level, with increased Nlrp3 and IL-1β protein expression in human podocytes (plenti v2 control cells), as demonstrated in **Figure 2B**. Interestingly, in human podocytes with CRISPR-Cas9-mediated Loxl2 knockdown, we observed a notable attenuation of Nlrp3 inflammasome activation. Specifically, the Loxl2 knockdown significantly reduced the LPS and high glucose-induced increase in Nlrp3 and IL-1β expression, at both the mRNA and protein levels. This indicates that Loxl2 plays a regulatory role in modulating the Nlrp3 inflammasome activity in response to inflammatory and hyperglycemic

conditions. These findings suggest that Loxl2 may serve as a key regulatory factor in preventing excessive Nlrp3 inflammasome activation, thereby potentially protecting podocytes from inflammatory damage and dysfunction, particularly under conditions relevant to diabetic nephropathy. By limiting the activation of the Nlrp3 inflammasome and the consequent production of pro-inflammatory cytokines, Loxl2 could play a protective role in maintaining podocyte health and mitigating glomerular damage. This novel insight into the interaction between Loxl2 and the Nlrp3 inflammasome in human podocytes highlights the potential of targeting Loxl2 as a therapeutic strategy for inflammatory and hyperglycemia-driven kidney diseases, such as diabetic nephropathy.

3.3 Loxl2 knockout reduces albuminuria in diabetic nephropathy

The Albumin-to-Creatinine Ratio (ACR), as presented in the figure, represents a critical biomarker for the assessment of renal function, particularly in the early detection of albuminuria(14). The ACR reflects the balance between the excretion of albumin and the concentration of creatinine in urine, offering a normalized measure of urinary albumin that accounts for variations in urine concentration. Elevated ACR levels typically indicate increased proteinuria, which serves as an early indicator of potential renal damage and is often used in clinical settings to monitor kidney function. This is especially relevant in patients with diabetes or hypertension, where ACR measurement aids in the early diagnosis of nephropathy, enabling timely intervention before more severe renal impairment develops.

The graph illustrates the differential ACR values, measured via ELISA, across various experimental groups, providing insights into the extent of renal dysfunction across the cohorts. Notable and statistically significant differences in ACR levels are observed between groups, reflecting varying degrees of renal impairment. Specifically, Nphs2-cre mice treated with streptozotocin (STZ) and the combination of STZ + high-fat diet (HFD) exhibited markedly elevated ACR values compared to the corresponding Nphs2-cre Loxl2 knockout (KO) mice subjected to the same treatments (STZ and STZ + HFD) (**Figure 3**).

These findings suggest that the deletion of the Loxl2 gene confers a protective effect against renal injury, as evidenced by the significantly attenuated ACR levels in the Loxl2 KO groups. The reduced ACR levels in Loxl2 KO mice indicate less albuminuria and, by extension, less renal damage in response to hyperglycemic and dietary stressors compared to wild-type mice. This protective effect highlights the potential role of Loxl2 in modulating pathways involved in renal injury, particularly

in the context of diabetic nephropathy. Consequently, Loxl2 may represent a promising therapeutic target for mitigating kidney damage in conditions characterized by elevated albuminuria, such as diabetes and metabolic syndrome.

3.4 Loxl2 expression was reduced in a mouse model of diabetic nephropathy

To explore the functional significance of podocyte-specific Loxl2 activation in the context of diabetic nephropathy (DN), Loxl2 knockout mice were generated with Cre recombinase expression driven specifically by the podocyte-specific Nphs2-Cre promoter, resulting in $Loxl2^{flox/flox}$ Podocin-Cre mice. This genetic approach allowed us to selectively delete Loxl2 in podocytes and to investigate whether Loxl2 activation in these cells is sufficient to exacerbate diabetic kidney disease (DKD). Experimental diabetes was induced by streptozotocin (STZ) injection (50 mg/kg, intraperitoneally), and a subset of mice was concurrently fed a high-fat diet (HFD) to simulate compounded metabolic stress, thereby establishing a robust model of diabetic kidney disease (DKD). Kidney tissues were harvested 24 weeks post-induction for molecular and histological evaluation(31). Quantitative real-time PCR analysis (**Figure 4A**) revealed that Loxl2 mRNA levels were significantly elevated in NPHS2-Cre (wild-type) mice subjected to STZ and STZ+HFD compared to vehicle controls, indicating transcriptional activation of Loxl2 in response to diabetic stress. In contrast, Loxl2 mRNA expression was effectively silenced in Nphs2-Cre Loxl2 knockout (KO) mice across all conditions, confirming efficient Cre-mediated recombination in podocytes. Western blot analysis (**Figure 4B**) corroborated these findings at the protein level, demonstrating a marked increase in Loxl2 protein abundance in diabetic NPHS2-Cre mice, particularly in the STZ+HFD group. As expected, Loxl2 protein was nearly undetectable in the kidneys of KO mice. Densitometric quantification (**Figure 4C**) further confirmed the statistical significance of these differences, validating the successful and specific knockout of Loxl2. Immunofluorescence staining (**Figure 4D**) provided spatial confirmation of Loxl2 expression, showing increased glomerular localization in NPHS2-Cre mice exposed to STZ and STZ+HFD. The Loxl2 signal colocalized with synaptopodin, a cytoskeletal marker specific to podocytes, indicating that diabetic stress induces Loxl2 upregulation primarily within these cells. In contrast, glomerular Loxl2 signal was virtually absent in Loxl2 KO mice across all treatment groups, confirming the specificity of deletion. Notably, synaptopodin staining remained detectable in both NPHS2-Cre and KO mice, even under diabetic conditions. This preservation of synaptopodin signal in KO mice reflects the intrinsic expression of

podocin driven by the Nphs2 promoter, which maintains podocyte identity independent of Loxl2 expression. Therefore, synaptopodin positivity in KO animals should not be interpreted as evidence of structural protection, but rather as a consequence of their genetic background. Together, these data demonstrate that Loxl2 is transcriptionally and translationally induced in podocytes in response to hyperglycemia and metabolic stress. The Nphs2-Cre; Loxl2$^{flox/flox}$ model provides a robust and specific platform for studying the cell-type–specific role of Loxl2 in podocyte biology and diabetic kidney disease progression. These findings indicate that Loxl2 may play a crucial role in the pathophysiology of diabetic nephropathy, particularly in mediating podocyte injury under hyperglycemic conditions. The upregulation of Loxl2 in diabetic nephropathy may exacerbate disease progression by contributing to podocyte dysfunction and loss(27). Therefore, targeting Loxl2 could represent a novel therapeutic strategy for mitigating the progression of diabetic nephropathy. Further research is warranted to fully elucidate the mechanisms by which Loxl2 contributes to podocyte injury and to explore its potential as a therapeutic target for the treatment of diabetic kidney disease.

3.5 Nlrp3 inflammasome expression is reduced in Loxl2 knockout diabetic nephropathy

In our study, streptozotocin (STZ)-induced diabetic mice exhibited a significant upregulation of Nlrp3 inflammasome expression, which was closely associated with increased inflammatory responses and exacerbated kidney injury(36, 40). The enhanced activation of the Nlrp3 inflammasome in diabetic conditions further underscores its role in driving inflammation and contributing to the pathogenesis of diabetic nephropathy(47). Interestingly, in Loxl2 knockout (KO) mice, STZ-induced hyperglycemia resulted in a marked reduction of Nlrp3 and Interleukin-1 beta (IL-1β) mRNA levels compared to wild-type controls, suggesting a protective role for Loxl2 deficiency in the context of diabetic nephropathy. Notably, despite the observed reductions at the mRNA level, there were no corresponding significant changes in the protein levels of Nlrp3 or IL-1β in the Loxl2 KO mice, indicating a possible post-transcriptional regulatory mechanism. These findings highlight a complex relationship between Loxl2 and Nlrp3 inflammasome activation in diabetic conditions, where Loxl2 appears to modulate Nlrp3 mRNA expression but may not fully suppress inflammasome activity at the protein level. Additionally, the expression of caspase-1, a key effector of the inflammasome complex, did not show significant changes in the Loxl2 KO mice,

similar to the results observed in our in vitro cell experiments. This consistent observation suggests that while Loxl2 influences Nlrp3 and IL-1β at the transcriptional level, its impact on the broader inflammasome activation pathway may be limited. Further investigation is required to clarify the regulatory mechanisms governing Nlrp3 activation at the protein level in Loxl2 KO mice and to determine the functional consequences of these changes in the progression of diabetic nephropathy. These results collectively highlight the potential involvement of the Nlrp3 inflammasome in the pathogenesis of STZ-induced diabetic kidney disease. Moreover, they underscore the important role of Loxl2 in modulating inflammasome activity and suggest that Loxl2 deficiency could serve as a protective mechanism against excessive inflammation and kidney damage in diabetic conditions. Future studies focusing on the protein-level regulation of the inflammasome will be essential to fully understand the therapeutic potential of targeting Loxl2 in diabetic nephropathy.

3.6 Podocyte-specific Loxl2 deficiency prevents maladaptive up-regulation of ACTN4

To investigate the impact of Loxl2 deletion on podocyte cytoskeletal integrity under diabetic conditions, we evaluated the expression of α-actinin4 (ACTN4) and synaptopodin, key markers of podocyte structure(48) by Western blot and immunofluorescence staining in kidney tissues from NPHS2-Cre (WT) and NPHS2-Cre Loxl2 knockout (KO) mice treated with vehicle, STZ, HFD, or STZ+HFD. Western blot analysis demonstrated that diabetic stress induced by STZ and STZ+HFD markedly increased ACTN4 expression in NPHS2-Cre mice compared to vehicle-treated controls (**Figure 6A**). This upregulation is interpreted as a compensatory cytoskeletal response to injury. In contrast, Loxl2 KO mice exhibited consistently low levels of ACTN4 expression across all treatment groups, including diabetic conditions. Quantitative densitometric analysis confirmed that ACTN4 expression was significantly lower in Loxl2 KO mice compared to NPHS2-Cre counterparts under diabetic conditions (**Figure 6B**). These results suggest that Loxl2 deficiency mitigates the cytoskeletal stress response in diabetic nephropathy. Immunofluorescence staining further validated these findings. In NPHS2-Cre mice, diabetic stress led to intense glomerular staining for ACTN4, while synaptopodin staining remained detectable but appeared more diffuse under STZ+HFD conditions (**Figure 6C**). In contrast, Loxl2 KO mice displayed diminished ACTN4 expression in glomeruli under diabetic conditions, with synaptopodin expression relatively preserved in morphology and intensity. The colocalization of ACTN4 and synaptopodin in merged images was

notably reduced in the Loxl2 KO group, suggesting altered cytoskeletal remodeling dynamics in the absence of Loxl2. Taken together, these data indicate that Loxl2 contributes to the cytoskeletal reorganization of podocytes in response to diabetic stress. Its deletion appears to protect against maladaptive upregulation of ACTN4 and helps maintain synaptopodin integrity, thereby preserving podocyte structural stability under diabetic conditions.

3.7 Loxl2 deficiency attenuates glomerular injury and inflammation in diabetic nephropathy

To evaluate structural and inflammatory changes in diabetic nephropathy and assess the protective role of Loxl2 deletion, we performed Periodic Acid–Schiff (PAS) staining and F4/80 immunohistochemistry on kidney sections from NPHS2-Cre (WT) and NPHS2-Cre Loxl2 knockout (KO) mice exposed to vehicle, streptozotocin (STZ), high-fat diet (HFD), or a combination of STZ and HFD. PAS staining revealed marked glomerular injury in diabetic NPHS2-Cre mice, particularly in the STZ and STZ+HFD groups. Characteristic pathological features included mesangial expansion, increased PAS-positive matrix deposition, and thickening of the glomerular basement membrane. These alterations are consistent with early structural remodeling seen in diabetic glomerulosclerosis. In contrast, Loxl2 KO mice exhibited substantial preservation of glomerular architecture across all diabetic conditions, with notably reduced mesangial expansion and matrix accumulation (**Figure 7A**). These findings suggest that Loxl2 deficiency mitigates diabetes-induced glomerular remodeling and matrix deposition. F4/80 immunohistochemistry, used to assess macrophage infiltration, showed elevated F4/80-positive staining in diabetic NPHS2-Cre mice, especially under STZ and STZ+HFD treatment. This reflects enhanced renal inflammation and immune cell recruitment in response to hyperglycemic and metabolic stress. However, Loxl2 KO mice demonstrated significantly reduced F4/80-positive cell infiltration in both glomerular and interstitial compartments (**Figure 7B**), indicating an attenuation of macrophage-mediated inflammatory responses. Collectively, these results indicate that podocyte-specific deletion of Loxl2 reduces both structural damage and inflammation in diabetic nephropathy. By preserving glomerular architecture and limiting macrophage infiltration, Loxl2 deficiency may provide a dual protective mechanism against the progression of diabetic kidney disease.

3.8 Loxl2 deficiency reduces renal fibrosis marker α-SMA expression in diabetic nephropathy.

To investigate the effect of Loxl2 deletion on renal fibrosis in diabetic nephropathy, we evaluated α-smooth muscle actin (α-SMA) expression by Western blot and immunohistochemistry in kidney tissues from NPHS2-Cre (WT) and NPHS2-Cre Loxl2 knockout (KO) mice subjected to vehicle, streptozotocin (STZ), high-fat diet (HFD), or combined STZ+HFD treatment. Western blot analysis demonstrated that α-SMA protein levels were significantly elevated in NPHS2-Cre mice under STZ treatment compared to vehicle controls, consistent with increased fibrogenic activation in diabetic nephropathy (**Figure 8A**). Quantification revealed a clear upregulation of α-SMA in diabetic conditions, whereas α-SMA levels remained relatively unchanged in Loxl2 KO mice across all treatment groups (**Figure 8B**). These results indicate that Loxl2 deletion suppresses diabetes-induced α-SMA expression. Immunohistochemical staining further supported these findings. In NPHS2-Cre mice, α-SMA staining was markedly increased in both glomerular and tubulointerstitial compartments following STZ, HFD, or STZ+HFD treatment, indicating enhanced activation of myofibroblasts and progression of renal fibrosis (**Figure 8C**). In contrast, kidney sections from Loxl2 KO mice exhibited substantially reduced α-SMA-positive staining, with minimal signal in both glomerular and interstitial areas, even under diabetic stress conditions. Together, these data suggest that Loxl2 plays a pivotal role in promoting renal fibrosis in diabetic nephropathy. Podocyte-specific deletion of Loxl2 attenuates the fibrotic response, as evidenced by reduced α-SMA expression, highlighting its potential as a therapeutic target for preventing renal fibrogenesis in diabetes.

A.

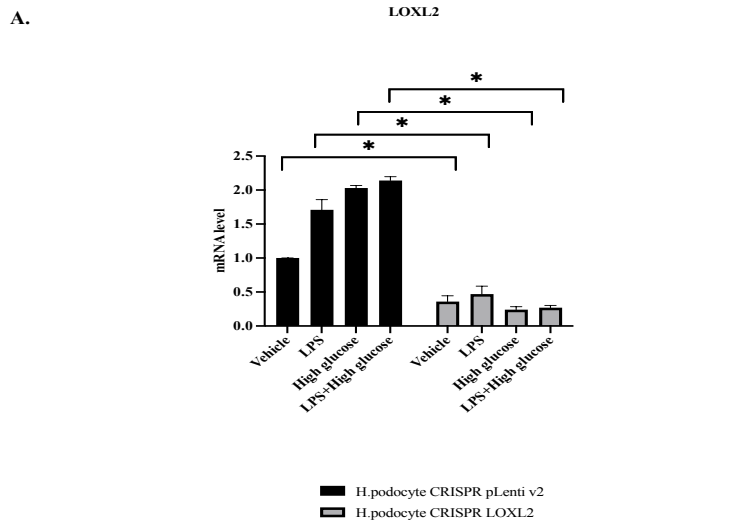

B.

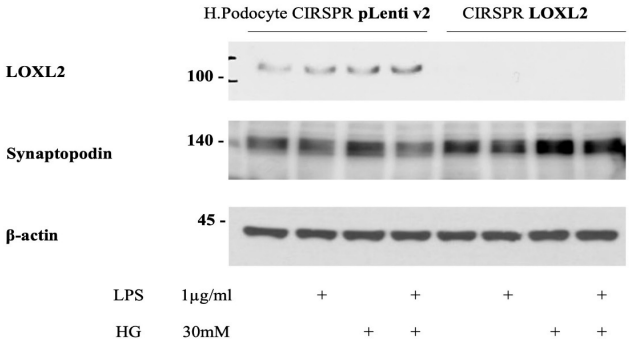

C.

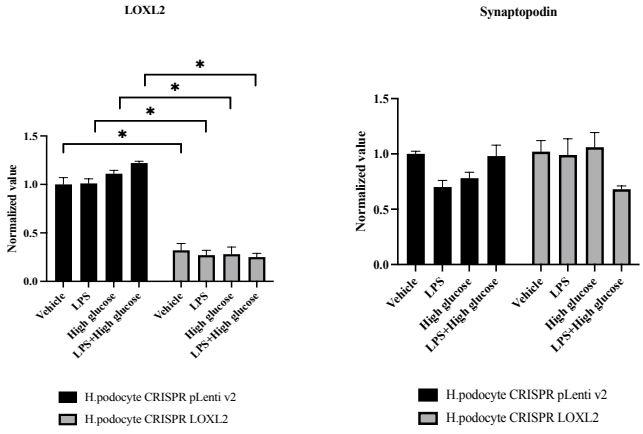

Figure 1. Loxl2 expression in podocytes under control and diabetic conditions.

(A) Quantitative real-time PCR shows that treatment with lipopolysaccharide (LPS, 1 μg ml^{-1}), high glucose (HG, 30 mM), or their combination (LPS + HG) significantly increases Loxl2 mRNA in control podocytes (plenti v2). In contrast, CRISPR-Cas9 Loxl2-knock-down cells maintain markedly lower Loxl2 transcripts under all conditions. (B) Representative Western blot confirms stimulus-dependent increases in Loxl2 protein in control cells, while Loxl2-KO cells show minimal signal; β-actin serves as a loading control. (C) Densitometric quantification demonstrates concordant protein up-regulation in control cells and effective suppression in KO cells. * $P < 0.05$ versus vehicle-treated controls.

A.

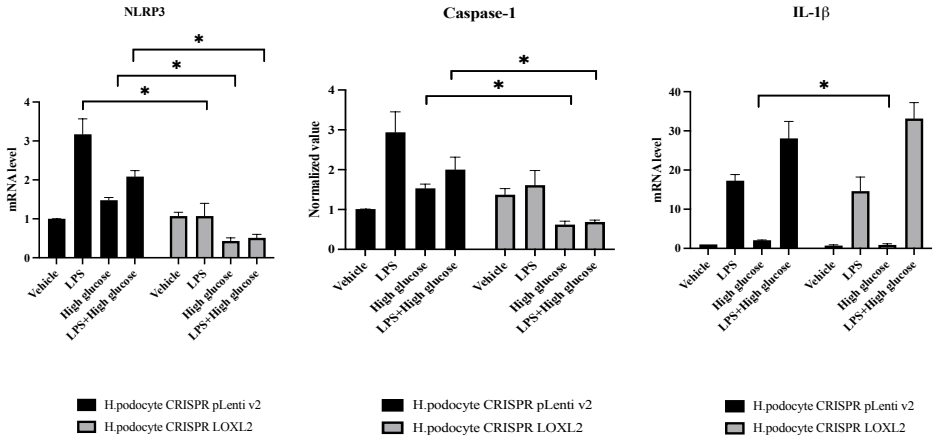

B.

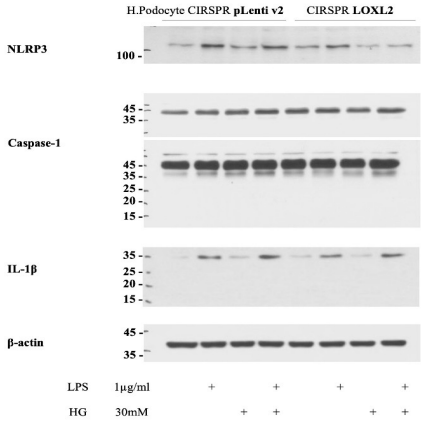

C.

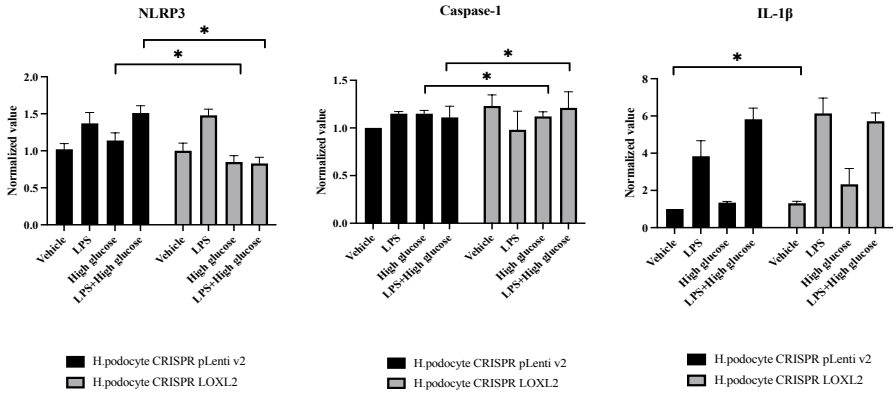

Figure 2. Knockdown (KD) of Loxl2 reduces Nlrp3 inflammasome expression in human podocytes.

(A) Quantitative real-time PCR analysis revealed that mRNA expression levels of Nlrp3 and Caspase-1 were significantly reduced in Loxl2 knockdown cells compared to vehicle-treated control cells. (B) Western blot analysis showing decreased protein levels of Nlrp3 and Caspase-1 in Loxl2 knockdown podocytes under high-glucose and inflammatory (LPS) conditions. (C) Band intensities from Western blot analyses were quantified using ImageJ software. β-actin was used as a loading control and was verified after stripping the Caspase-1 blot. Data are presented as mean ± standard error of the mean (SEM) from three independent experiments. Statistical significance was determined using an unpaired two-tailed Student's t-test. $*P < 0.05$ was considered statistically significant.

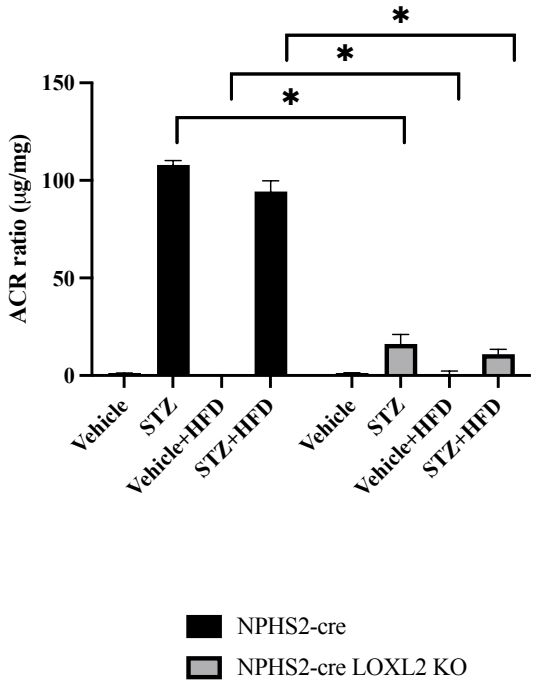

Figure 3. Level of urinary albumin/creatinine ratio (ACR) in Nphs2-cre and Nphs2-cre Loxl2 KO mice.

Urinary albumin/creatinine ratio (ACR) was measured in the final week of the experiment using an ELISA-based method to assess albuminuria in each group. Data are presented as mean ± standard error of the mean (SEM) from 4–5 mice per group. Statistical significance was determined using an unpaired two-tailed Student's t-test. *$P < 0.05$ was considered statistically significant.

A.

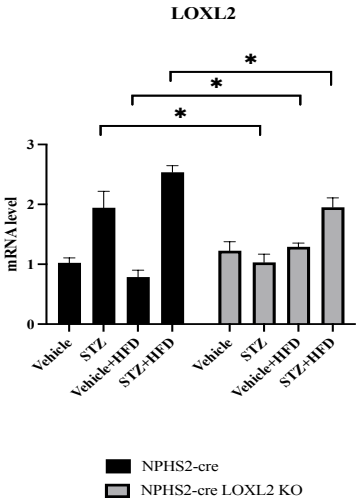

B.

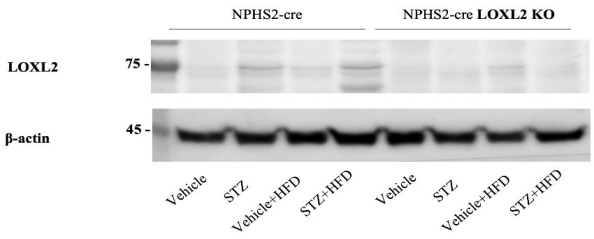

C.

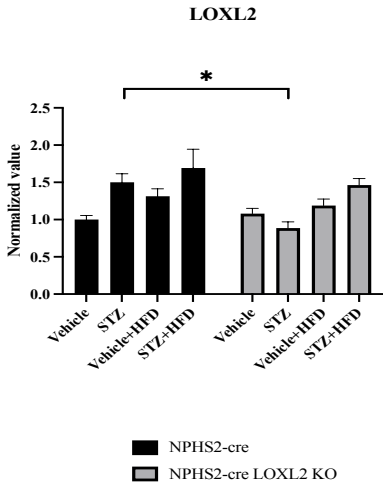

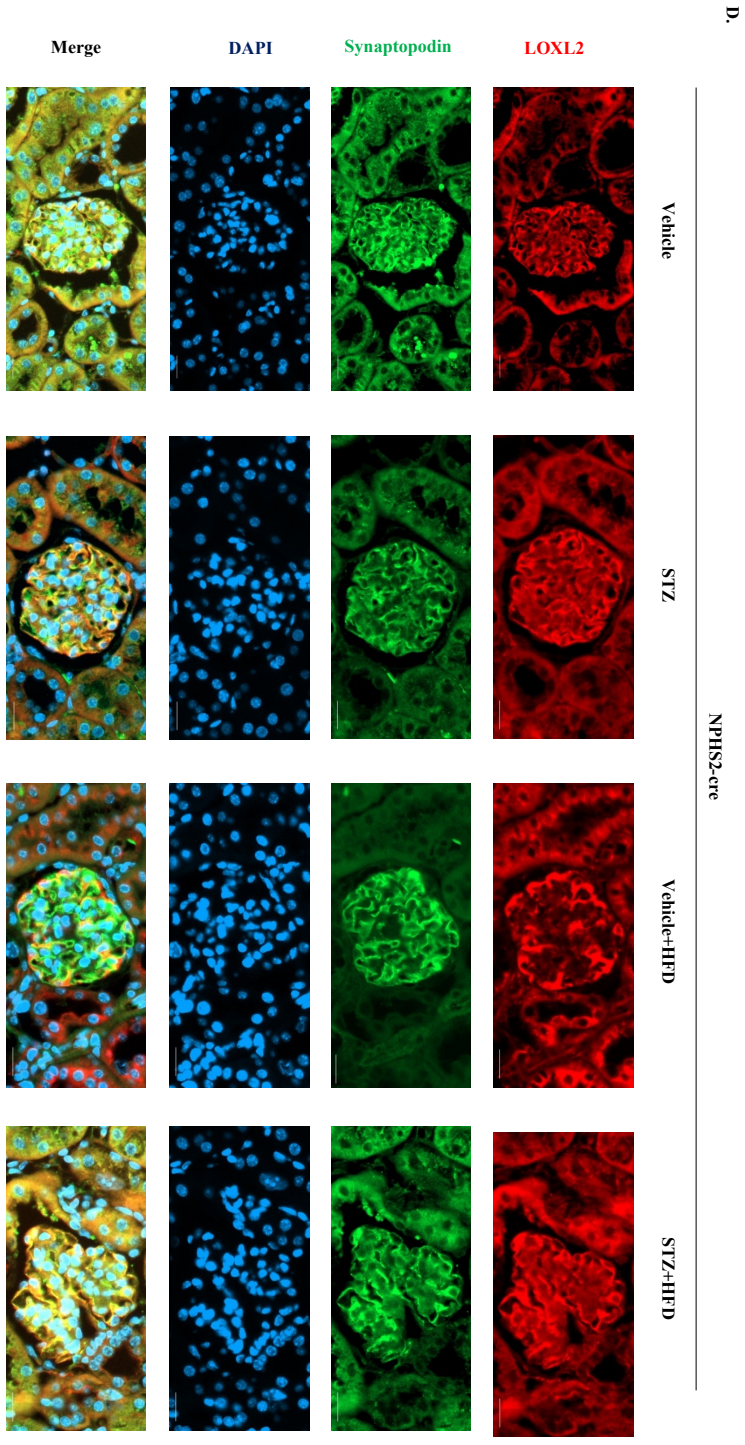

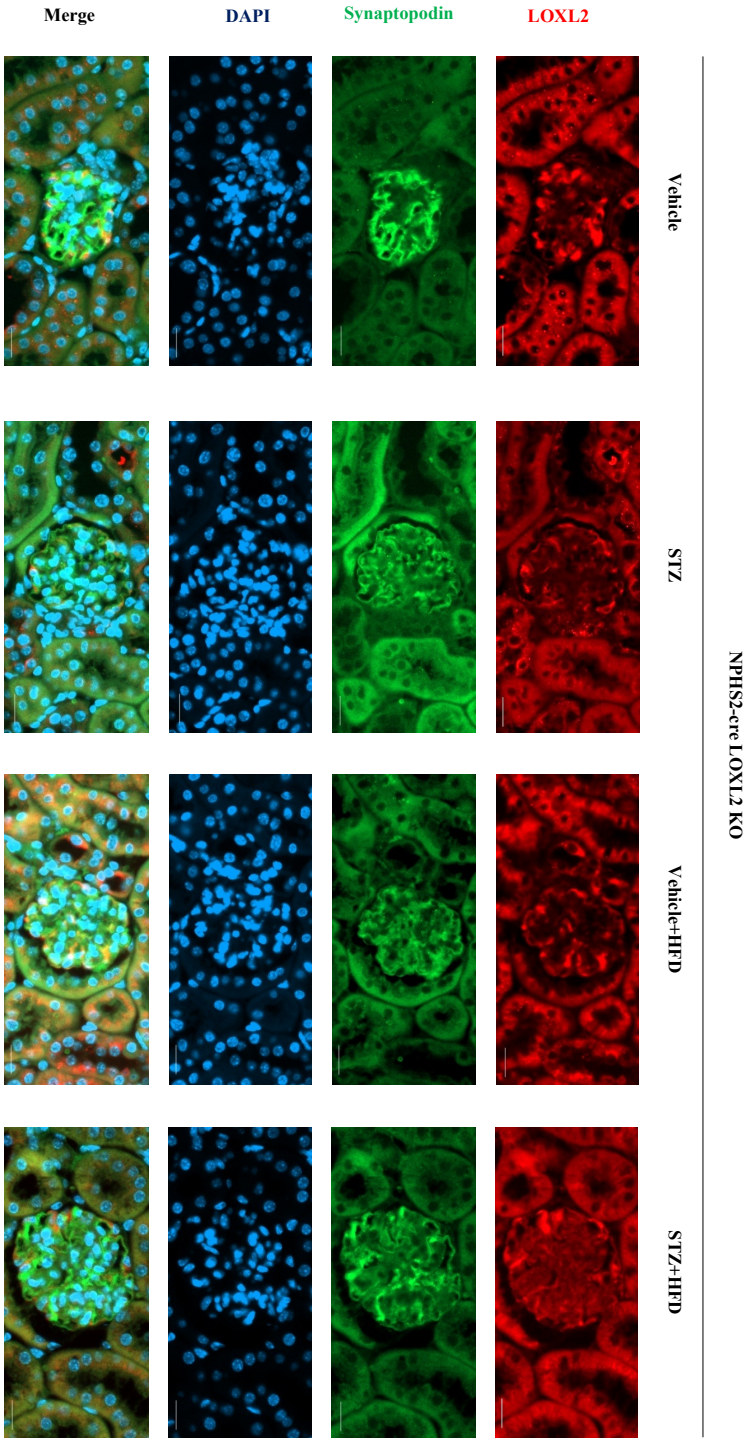

Figure 4. Podocyte-specific Loxl2 deficiency protects against diabetic kidney disease (DKD).

Relative Loxl2 expression levels were compared between wild-type (Nphs2-cre) and podocyte-specific Loxl2 knockout (Nphs2-cre Loxl2 KO) mice. STZ and high-fat diet (HFD) treatment led to upregulation of Loxl2 mRNA (A) and protein expression (B) in wild-type mice. In contrast, Loxl2 expression was markedly reduced in Loxl2 KO mice as expected. (C) Quantification of Western blot band intensities. (D) Immunofluorescence staining showed Loxl2 expression localized to glomeruli in wild-type mice, which was markedly diminished in Loxl2 KO mice. Sections were stained for Loxl2 (red), Synaptopodin (green), and nuclei (blue, DAPI). Merged images demonstrate the colocalization of Loxl2 with podocyte markers. Images were captured at 200× magnification, scale bar = 20 μm. Data are presented as mean ± standard error of the mean (SEM) from 4–5 mice per group. Statistical significance was determined using an unpaired two-tailed Student's t-test. $*P < 0.05$ was considered statistically significant.

A.

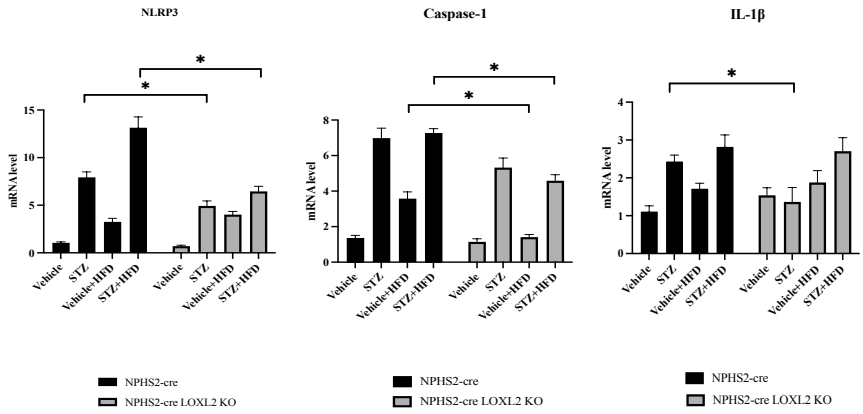

B.

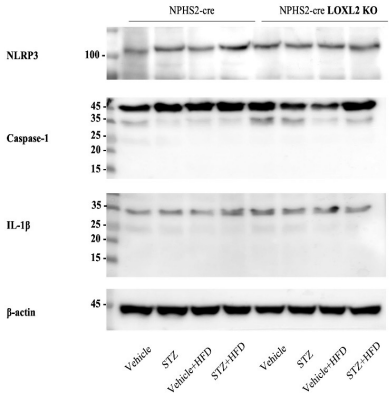

C.

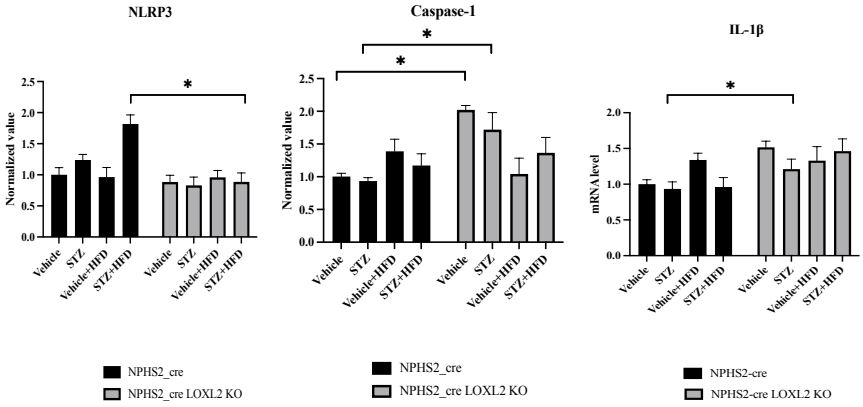

Figure 5. Nlrp3 inflammasome expression is reduced in Loxl2 knockout mice with diabetic nephropathy.

(A–C) Quantitative real-time PCR analysis of renal mRNA expression levels of Nlrp3 (A), Caspase-1 (B), and Il-1β (C) in NPHS2-cre and NPHS2-cre Loxl2 knockout (KO) mice following treatment with vehicle, STZ, high-fat diet (HFD), or a combination of STZ and HFD. Diabetic stress conditions upregulated inflammasome-related gene expression in wild-type mice, which was attenuated in Loxl2 KO mice. (D) Representative Western blot images showing protein expression of Nlrp3, Caspase-1, and IL-1β in kidney tissue lysates from each group. (E–G) Densitometric quantification of Western blot results for Nlrp3 (E), Caspase-1 (F), and IL-1β (G), normalized to β-actin. Inflammasome activation was significantly reduced in Loxl2 KO mice compared to NPHS2-cre mice under diabetic conditions. Data are presented as mean ± standard error of the mean (SEM) from 4–5 mice per group. Statistical significance was determined using an unpaired two-tailed Student's t-test. *$P < 0.05$ was considered statistically significant.

A.

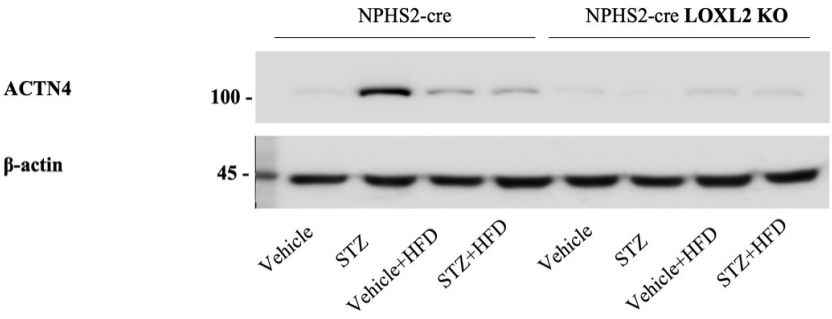

B.

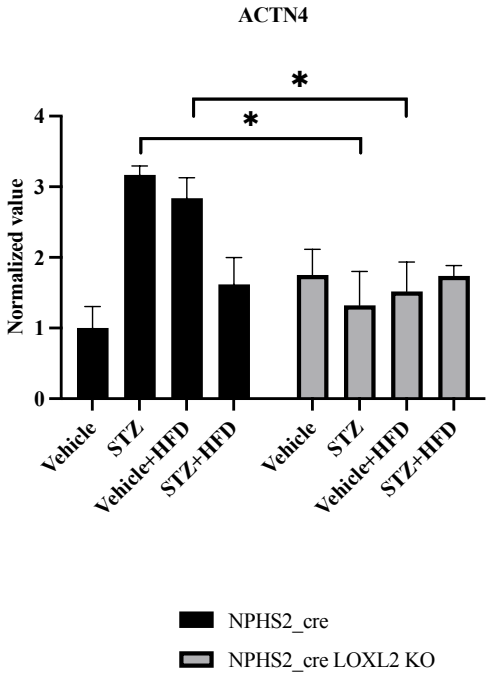

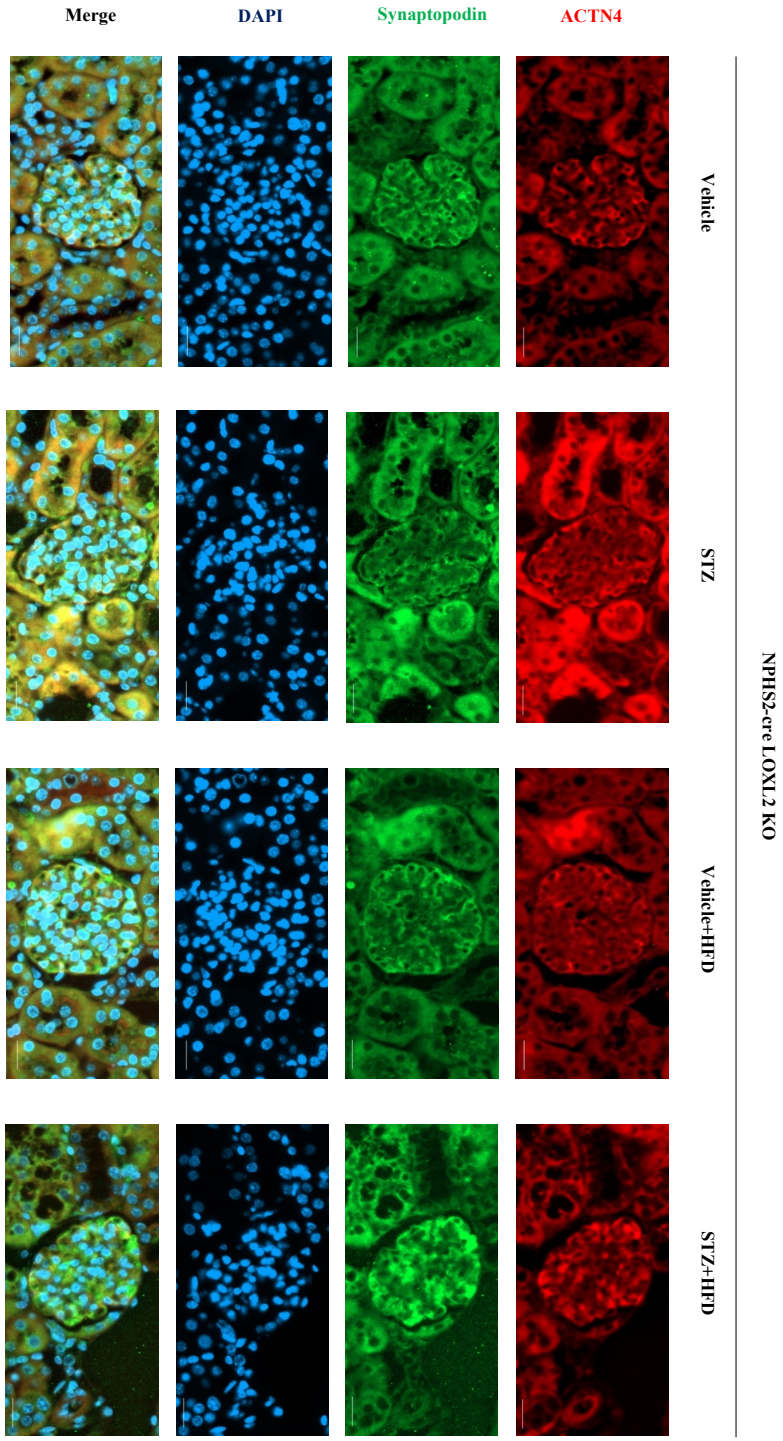

Figure 6. Podocyte-specific Loxl2 deletion prevents maladaptive up-regulation of ACTN4 in diabetic glomeruli.

(A) Western blot analysis of ACTN4 protein levels in kidney tissue lysates from NPHS2-cre and NPHS2-cre Loxl2 knockout (KO) mice treated with vehicle, STZ, HFD, or STZ+HFD. β-actin was used as a loading control. (B) Densitometric quantification of ACTN4 band intensities normalized to β-actin. ACTN4 expression was increased in NPHS2-cre mice under STZ and STZ+HFD conditions, whereas Loxl2 KO mice exhibited relatively preserved or stable ACTN4 levels across all groups. (C) Immunofluorescence staining of kidney sections for ACTN4 (red), Synaptopodin (green; a podocyte-specific marker), and nuclei (DAPI, blue). In NPHS2-cre mice, ACTN4 signal intensity increased under diabetic conditions, indicating podocyte cytoskeletal stress. In contrast, Loxl2 KO mice maintained consistent and less aberrant ACTN4 distribution across all treatment conditions. Merged images show colocalization of ACTN4 and Synaptopodin in the glomeruli. Images were acquired at 200× magnification; scale bar = 20 μm. Data are presented as mean ± standard error of the mean (SEM) from 5 mice per group. Statistical significance was determined using an unpaired two-tailed Student's t-test. $*P < 0.05$ was considered statistically significant.

A.

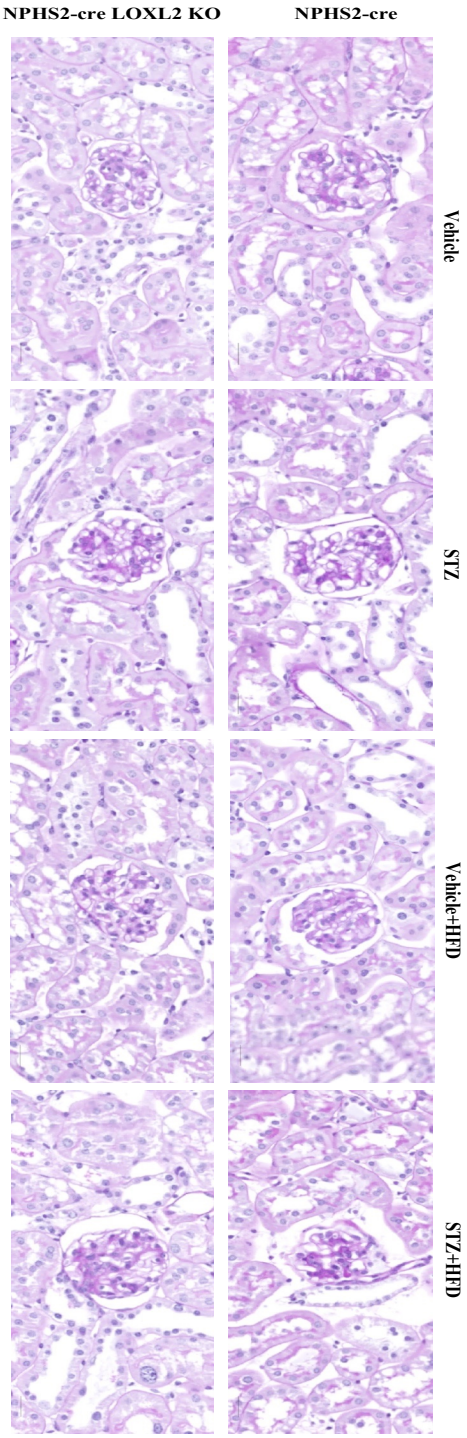

B.

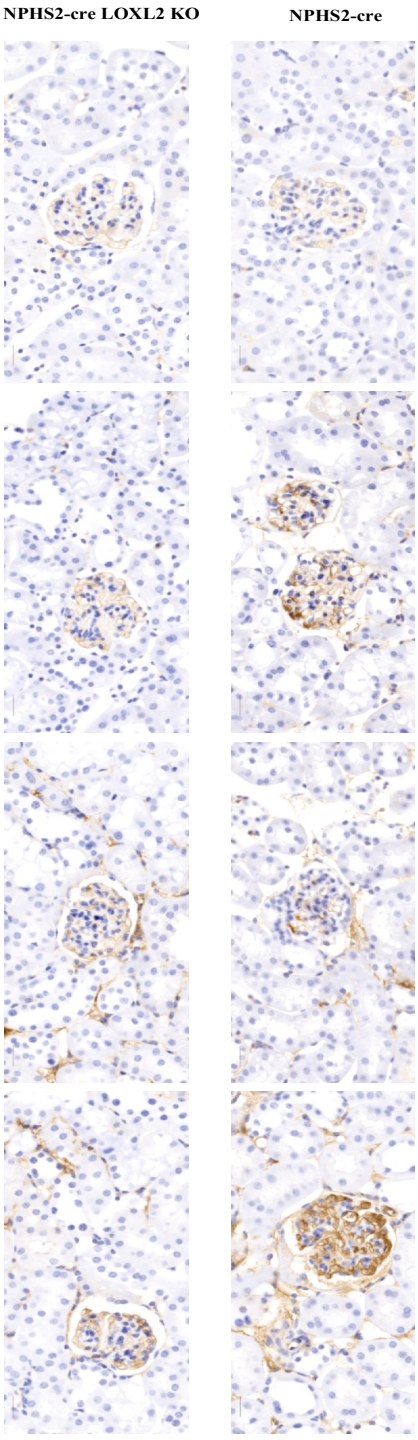

Figure 7. Loxl2 deletion reduces renal inflammation but does not significantly alter glomerular morphology in diabetic nephropathy.

(A) Periodic Acid–Schiff (PAS) staining of kidney sections from NPHS2-cre and NPHS2-cre Loxl2 knockout (KO) mice treated with vehicle, STZ, HFD, or STZ+HFD. Across all groups, including diabetic conditions, there were no marked differences in glomerular morphology between NPHS2-cre and Loxl2 KO mice. Mesangial expansion and matrix deposition appeared comparable, suggesting that Loxl2 deletion did not significantly affect structural glomerular injury as assessed by PAS staining. (B) F4/80 immunohistochemistry was performed to assess renal macrophage infiltration. In NPHS2-cre mice, STZ and STZ+HFD conditions induced increased F4/80-positive cell infiltration, indicative of enhanced renal inflammation. This inflammatory response was notably attenuated in Loxl2 KO mice, with fewer F4/80-positive cells observed in both glomerular and interstitial areas. Images were acquired at 200× magnification; scale bar = 20 μm. Data are representative of 2-3 mice per group. Morphological and immunohistochemical findings were consistent across biological replicates.

A.

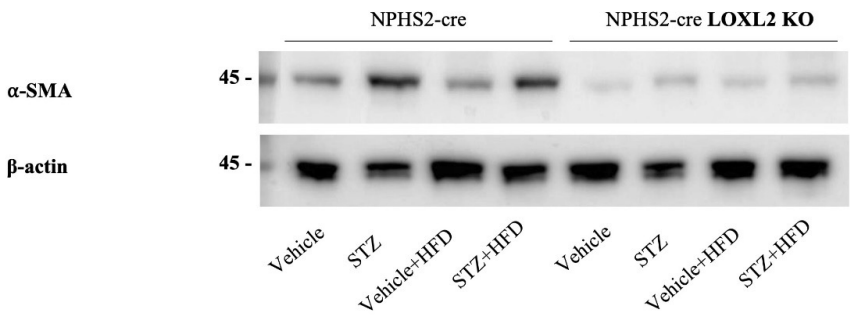

B.

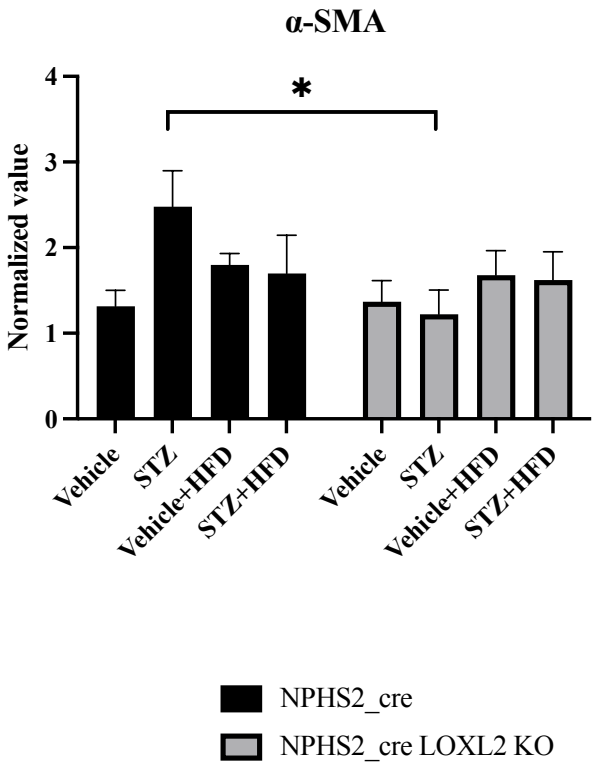

c.

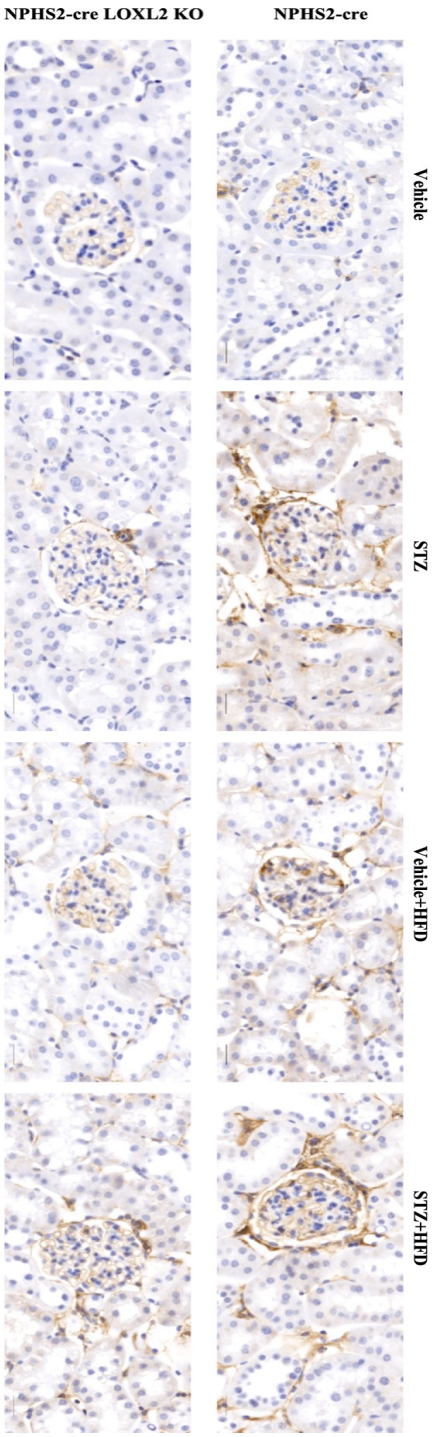

Figure 8. Loxl2 deletion reduces renal fibrosis marker α-SMA expression in diabetic nephropathy.

(A) Western blot analysis of α-SMA protein levels in kidney lysates from NPHS2-cre and NPHS2-cre Loxl2 knockout (KO) mice treated with vehicle, STZ, HFD, or STZ+HFD. Diabetic NPHS2-cre mice showed increased α-SMA expression, whereas Loxl2 KO mice displayed markedly reduced expression across all treatment conditions. β-actin was used as a loading control. (B) Densitometric quantification of α-SMA protein levels normalized to β-actin. STZ treatment significantly increased α-SMA expression in NPHS2-cre mice, while this response was attenuated in Loxl2 KO mice. (C) Immunohistochemical staining for α-SMA in kidney tissue. STZ and STZ+HFD treatment in NPHS2-cre mice resulted in stronger α-SMA staining in both glomerular and interstitial compartments, indicative of fibrosis. In contrast, Loxl2 KO mice exhibited weaker α-SMA staining under all conditions, suggesting a protective effect against fibrotic remodeling. Images were acquired at 200× magnification; scale bar = 20 μm. Data are presented as mean ± standard error of the mean (SEM) from 5 mice per group. Statistical significance was determined using an unpaired two-tailed Student's t-test. $*P < 0.05$ was considered statistically significant.

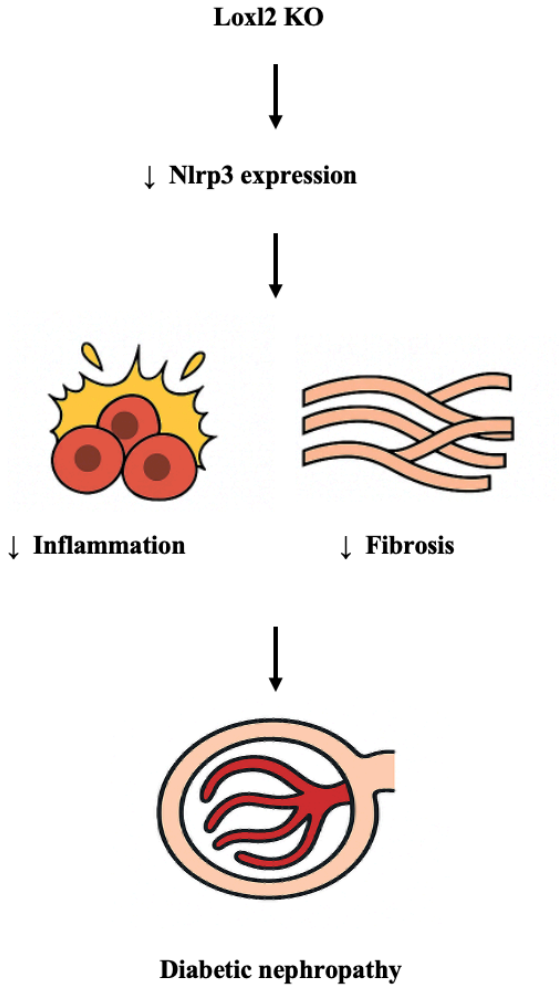

Figure 9. Proposed mechanism of Loxl2 knockout-mediated protection against diabetic nephropathy

Schematic illustration of the molecular pathway by which NPHS2-cre Loxl2 knockout (KO) alleviates diabetic nephropathy. NPHS2-cre Loxl2 knockout (KO) leads to decreased expression of

Nlrp3, a key component of the inflammasome complex. This suppression results in the reduction of inflammation and fibrosis within glomerular structures, ultimately mitigating the progression of diabetic nephropathy. The diagram summarizes the hypothesized mechanism derived from in vitro and in vivo experimental results demonstrating Loxl2's role in regulating Nlrp3-dependent inflammatory and fibrotic responses in podocytes under diabetic conditions.

4. Discussion

Diabetic nephropathy (DN) is a principal microvascular complication of diabetes and a leading cause of end-stage renal disease (ESRD) worldwide(5, 37). It is characterized by progressive damage to various renal compartments, including the glomeruli, tubules, interstitium, and vasculature(9, 49). Among these, early glomerular injury, particularly affecting podocytes, is central to the pathogenesis of DN(1, 15, 50). Podocytes, terminally differentiated epithelial cells of the glomerular filtration barrier, are vulnerable to hyperglycemia-induced injury(4, 51). Podocyte loss and dysfunction manifest as foot process effacement, loss of slit diaphragm integrity, and ultimately, proteinuria and glomerulosclerosis(51, 52). Mounting evidence indicates that preservation of podocyte structure and function is crucial for halting the progression of DN.

In this study, we identified lysyl oxidase-like 2 (Loxl2) as a significant mediator of podocyte injury under diabetic stress. Loxl2 is a member of the LOX family of copper-dependent amine oxidases that catalyze the cross-linking of extracellular matrix (ECM) proteins, such as collagen and elastin(20, 26). Beyond its enzymatic role, Loxl2 has been implicated in diverse pathological processes including fibrosis, epithelial-to-mesenchymal transition (EMT), and tissue remodeling. Previous studies have highlighted Loxl2 as a key contributor to fibrogenesis in hepatic and pulmonary models, but its role in renal fibrosis particularly in the context of DN has remained poorly understood.

Our results demonstrate that both in vitro and in vivo diabetic conditions upregulate Loxl2 expression in podocytes. Human podocytes exposed to high glucose and inflammatory stimuli exhibited increased Loxl2 mRNA and protein levels. In mouse models, Loxl2 expression was significantly elevated in glomeruli following STZ and STZ + HFD treatment. Notably, podocyte-specific deletion of Loxl2 led to attenuation of hallmark features of DN, including mesangial expansion, matrix accumulation, and glomerular basement membrane (GBM) thickening(23). This suggests that Loxl2 directly contributes to the structural remodeling of glomeruli via ECM dysregulation.

In addition to its structural role, Loxl2 also appears to influence inflammatory signaling pathways. We observed that Loxl2 knockdown significantly suppressed the expression of Nlrp3 inflammasome components, including Nlrp3 and IL-1β, at both the mRNA and protein levels. The Nlrp3 inflammasome is a key mediator of sterile inflammation in DN, activated by metabolic stressors such as hyperglycemia, ROS, and AGEs. Its activation leads to the maturation of pro-inflammatory

cytokines and contributes to podocyte injury, macrophage infiltration, and tubulointerstitial fibrosis(33, 34, 38, 41, 53, 54). The attenuation of Nlrp3 inflammasome activity in Loxl2-deficient podocytes implies a regulatory interaction between fibrotic and inflammatory pathways.

Interestingly, Loxl2 deletion also mitigated cytoskeletal alterations in podocytes(55, 56). Under diabetic stress, ACTN4 (alpha-actinin-4) expression was upregulated, indicating cytoskeletal reorganization and stress response(48, 57). However, in Loxl2 KO mice, ACTN4 expression was significantly reduced, while synaptopodin an actin-associated marker of mature podocytes was preserved. These findings suggest that Loxl2 contributes to cytoskeletal instability under diabetic conditions, potentially through ECM-cytoskeleton cross-talk or EMT-like signaling.

Moreover, Loxl2 deficiency led to reduced macrophage infiltration (F4/80) and diminished α-SMA expression, a marker of myofibroblast activation and fibrosis(31, 32, 58). These observations collectively underscore the multifaceted role of Loxl2 in orchestrating ECM remodeling, inflammation, and cytoskeletal regulation in DN. They support the hypothesis that targeting Loxl2 in podocytes may offer dual protective effects by preserving glomerular architecture and modulating inflammatory cascades.

While our findings are compelling, several questions remain. The precise molecular mechanisms by which Loxl2 regulates Nlrp3 signaling are unclear. It is possible that Loxl2 influences upstream modulators such as NF-κB, TGF-β, or ROS, which are known to impact inflammasome priming(3, 33, 38, 59). Alternatively, Loxl2 may affect ECM stiffness or cellular stress responses that indirectly modulate inflammasome activation(33, 60-62). Further studies employing transcriptomic, proteomic, and single-cell resolution analyses will be necessary to delineate these interactions.

In addition, the current study focused exclusively on podocytes. Given the expression of Loxl2 in mesangial and tubular epithelial cells(27, 31), cell-type specific knockout or lineage tracing models are warranted to explore the broader impact of Loxl2 in renal fibrosis and DN progression(31, 32, 63). Furthermore, the translational potential of pharmacological Loxl2 inhibition should be explored in future studies, using both small molecules and monoclonal antibodies. Such interventions may provide a viable therapeutic approach for DN without the need for genetic modification.

In summary, our study identifies Loxl2 as a novel regulator of podocyte injury in diabetic nephropathy. Through its dual roles in ECM remodeling and inflammasome activation, Loxl2 contributes to glomerular dysfunction, inflammation, and fibrosis. Podocyte-specific deletion of Loxl2 confers significant renoprotective effects, supporting its candidacy as a therapeutic target.

These findings expand our understanding of DN pathogenesis and pave the way for future mechanistic and translational investigations.

5. Conclusion

In conclusion, this study provides compelling evidence that lysyl oxidase-like 2 (Loxl2) plays a critical role in the development and progression of diabetic nephropathy (DN), primarily through its actions in podocytes. We demonstrated that Loxl2 expression is markedly upregulated under diabetic conditions, both in vitro and in vivo, and that podocyte-specific deletion of Loxl2 significantly mitigates the pathological features of DN. These include a reduction in albuminuria, decreased expression of pro-fibrotic markers such as α-SMA, diminished activation of the Nlrp3 inflammasome, and preservation of podocyte-specific cytoskeletal proteins including synaptopodin and α-actinin4(ACTN4).

Our findings support the notion that Loxl2 contributes not only to extracellular matrix (ECM) cross-linking and fibrotic remodeling but also to the inflammatory milieu characteristic of diabetic kidney injury. By modulating both structural and immunological pathways, Loxl2 appears to be a central mediator of podocyte injury. The attenuation of inflammasome activation in Loxl2-deficient models further highlights a novel axis of interaction between ECM remodeling enzymes and innate immune sensors.

The study's integration of genetic models, molecular analyses, and histopathological evaluation provides a comprehensive understanding of Loxl2's impact. Importantly, our results offer a strong rationale for targeting Loxl2 as a therapeutic strategy for diabetic nephropathy. Inhibition of Loxl2, either genetically or pharmacologically, may confer dual benefits by reducing both fibrosis and inflammation.

Future investigations should explore the cell-type–specific roles of Loxl2 in other compartments of the nephron, as well as its interaction with other fibrogenic and inflammatory pathways. The use of single-cell transcriptomics, proteomics, and in vivo pharmacological inhibitors will be instrumental in delineating the full therapeutic potential of Loxl2 inhibition.

Ultimately, this study contributes to the growing body of evidence that supports Loxl2 as a promising therapeutic target in DN, potentially opening new avenues for the development of more effective treatments for patients suffering from diabetes-associated kidney disease.

References

1. Azushima K, Gurley SB, Coffman TM. Modelling diabetic nephropathy in mice. Nat Rev Nephrol. 2018;14(1):48-56.

2. Huang R, Fu P, Ma L. Kidney fibrosis: from mechanisms to therapeutic medicines. Signal Transduct Target Ther. 2023;8(1):129.

3. An DY, Tan J, Lu YD, Wen ZH, Bao YN, Yao ZH, et al. Focus on podocytes: diabetic kidney disease and renal fibrosis - a global bibliometric analysis (2000-2024). Front Pharmacol. 2024;15:1454586.

4. Asanuma K, Mundel P. The role of podocytes in glomerular pathobiology. Clin Exp Nephrol. 2003;7(4):255-9.

5. Huang G, Zhang Y, Zhang Y, Ma Y. Chronic kidney disease and NLRP3 inflammasome: Pathogenesis, development and targeted therapeutic strategies. Biochem Biophys Rep. 2023;33:101417.

6. Kendall RT, Feghali-Bostwick CA. Fibroblasts in fibrosis: novel roles and mediators. Front Pharmacol. 2014;5:123.

7. Saleem MA, O'Hare MJ, Reiser J, Coward RJ, Inward CD, Farren T, et al. A conditionally immortalized human podocyte cell line demonstrating nephrin and podocin expression. J Am Soc Nephrol. 2002;13(3):630-8.

8. Hu S, Hang X, Wei Y, Wang H, Zhang L, Zhao L. Crosstalk among podocytes, glomerular endothelial cells and mesangial cells in diabetic kidney disease: an updated review. Cell Commun Signal. 2024;22(1):136.

9. Abbate M, Zoja C, Remuzzi G. How does proteinuria cause progressive renal damage? J Am Soc Nephrol. 2006;17(11):2974-84.

10. Lennon R, Randles MJ, Humphries MJ. The importance of podocyte adhesion for a healthy glomerulus. Front Endocrinol (Lausanne). 2014;5:160.

11. Li X, Zhang Y, Xing X, Li M, Liu Y, Xu A, et al. Podocyte injury of diabetic nephropathy: Novel mechanism discovery and therapeutic prospects. Biomed Pharmacother. 2023;168:115670.

12. Kravets I, Mallipattu SK. The Role of Podocytes and Podocyte-Associated Biomarkers in Diagnosis and Treatment of Diabetic Kidney Disease. J Endocr Soc. 2020;4(4):bvaa029.

13. Hofherr A, Williams J, Gan LM, Soderberg M, Hansen PBL, Woollard KJ. Targeting inflammation for the treatment of Diabetic Kidney Disease: a five-compartment mechanistic model. BMC Nephrol. 2022;23(1):208.

14. Cholongitas E, Goulis I, Ioannidou M, Soulaidopoulos S, Chalevas P, Akriviadis E. Urine albumin-to-creatinine ratio is associated with the severity of liver disease, renal function and survival in patients with decompensated cirrhosis. Hepatol Int. 2017;11(3):306-14.

15. Fioretto P, Mauer M. Histopathology of diabetic nephropathy. Semin Nephrol. 2007;27(2):195-207.

16. Balkawade RS, Chen C, Crowley MR, Crossman DK, Clapp WL, Verlander JW, et al. Podocyte-specific expression of Cre recombinase promotes glomerular basement membrane thickening. Am J Physiol Renal Physiol. 2019;316(5):F1026-F40.

17. Barker HE, Chang J, Cox TR, Lang G, Bird D, Nicolau M, et al. LOXL2-mediated matrix remodeling in metastasis and mammary gland involution. Cancer Res. 2011;71(5):1561-72.

18. Umana-Diaz C, Pichol-Thievend C, Marchand MF, Atlas Y, Salza R, Malbouyres M, et al. Scavenger Receptor Cysteine-Rich domains of Lysyl Oxidase-Like2 regulate endothelial ECM and angiogenesis through non-catalytic scaffolding mechanisms. Matrix Biol. 2020;88:33-52.

19. Wen B, Xu LY, Li EM. LOXL2 in cancer: regulation, downstream effectors and novel roles. Biochim Biophys Acta Rev Cancer. 2020;1874(2):188435.

20. Zhang X, Wang Q, Wu J, Wang J, Shi Y, Liu M. Crystal structure of human lysyl oxidase-like 2 (hLOXL2) in a precursor state. Proc Natl Acad Sci U S A. 2018;115(15):3828-33.

21. Nishioka T, Eustace A, West C. Lysyl oxidase: from basic science to future cancer treatment. Cell Struct Funct. 2012;37(1):75-80.

22. Peinado H, Moreno-Bueno G, Hardisson D, Perez-Gomez E, Santos V, Mendiola M, et al. Lysyl oxidase-like 2 as a new poor prognosis marker of squamous cell carcinomas. Cancer Res. 2008;68(12):4541-50.

23. Chen J, Ren J, Loo WTY, Hao L, Wang M. Lysyl oxidases expression and histopathological changes of the diabetic rat nephron. Mol Med Rep. 2018;17(2):2431-41.

24. Wang H, Poe A, Martinez Yus M, Pak L, Nandakumar K, Santhanam L. Lysyl oxidase-like 2 processing by factor Xa modulates its activity and substrate preference. Commun Biol. 2023;6(1):375.

25. Cano A, Santamaria PG, Moreno-Bueno G. LOXL2 in epithelial cell plasticity and tumor progression. Future Oncol. 2012;8(9):1095-108.

26. Cuevas EP, Moreno-Bueno G, Canesin G, Santos V, Portillo F, Cano A. LOXL2 catalytically inactive mutants mediate epithelial-to-mesenchymal transition. Biol Open. 2014;3(2):129-37.

27. Choi SE, Jeon N, Choi HY, Shin JI, Jeong HJ, Lim BJ. Lysyl oxidase-like 2 is expressed in kidney tissue and is associated with the progression of tubulointerstitial fibrosis. Mol Med Rep. 2017;16(3):2477-82.

28. Erasmus M, Samodien E, Lecour S, Cour M, Lorenzo O, Dludla P, et al. Linking LOXL2 to Cardiac Interstitial Fibrosis. Int J Mol Sci. 2020;21(16).

29. Lu Y, Li H, Chen M, Lin Y, Zhang X. LOX-induced tubulointerstitial fibrosis via the TGF-beta/LOX/Snail axis in diabetic mice. J Transl Med. 2025;23(1):35.

30. Cosgrove D, Dufek B, Meehan DT, Delimont D, Hartnett M, Samuelson G, et al. Lysyl oxidase like-2 contributes to renal fibrosis in Col4alpha3/Alport mice. Kidney Int. 2018;94(2):303-14.

31. Stangenberg S, Saad S, Schilter HC, Zaky A, Gill A, Pollock CA, et al. Lysyl oxidase-like 2 inhibition ameliorates glomerulosclerosis and albuminuria in diabetic nephropathy. Sci Rep. 2018;8(1):9423.

32. Tan K, Deng J, Liu Y, Zhang Y, Xiong Y, Yuan S, et al. Yiqi Juanshen decoction alleviates renal interstitial fibrosis by targeting the LOXL2/PI3K/AKT pathway to suppress EMT and inflammation. Sci Rep. 2025;15(1):4248.

33. Satheesan A, Kumar J, Leela KV, Murugesan R, Chaithanya V, Angelin M. Review on the role of nucleotide-binding oligomerization domain-like receptor protein 3 (NLRP3) inflammasome pathway in diabetes: mechanistic insights and therapeutic implications. Inflammopharmacology. 2024;32(5):2753-79.

34. Tang SCW, Yiu WH. Innate immunity in diabetic kidney disease. Nat Rev Nephrol. 2020;16(4):206-22.

35. Wang MZ, Wang J, Cao DW, Tu Y, Liu BH, Yuan CC, et al. Fucoidan Alleviates Renal Fibrosis in Diabetic Kidney Disease via Inhibition of NLRP3 Inflammasome-Mediated Podocyte Pyroptosis. Front Pharmacol. 2022;13:790937.

36. Hou Y, Lin S, Qiu J, Sun W, Dong M, Xiang Y, et al. NLRP3 inflammasome negatively regulates podocyte autophagy in diabetic nephropathy. Biochem Biophys Res Commun. 2020;521(3):791-8.

37. Ram C, Jha AK, Ghosh A, Gairola S, Syed AM, Murty US, et al. Targeting NLRP3 inflammasome as a promising approach for treatment of diabetic nephropathy: Preclinical evidences with therapeutic approaches. Eur J Pharmacol. 2020;885:173503.

38. Qiu YY, Tang LQ. Roles of the NLRP3 inflammasome in the pathogenesis of diabetic nephropathy. Pharmacol Res. 2016;114:251-64.

39. Ji Y, Hua H, Jia Z, Zhang A, Ding G. Therapy Targeted to the NLRP3 Inflammasome in Chronic Kidney Disease. Kidney Dis (Basel). 2024;10(5):369-83.

40. Sun L, Ding M, Chen F, Zhu D, Xie X. Breviscapine alleviates podocyte injury by inhibiting NF-kappaB/NLRP3-mediated pyroptosis in diabetic nephropathy. PeerJ. 2023;11:e14826.

41. Shahzad K, Fatima S, Khawaja H, Elwakiel A, Gadi I, Ambreen S, et al. Podocyte-specific Nlrp3 inflammasome activation promotes diabetic kidney disease. Kidney Int. 2022;102(4):766-79.

42. Saito AC, Higashi T, Chiba H. Protocol for establishing knockout cell clones by deletion of a large gene fragment using CRISPR-Cas9 with multiple guide RNAs. STAR Protoc. 2024;5(3):103179.

43. Mundel P, Heid HW, Mundel TM, Kruger M, Reiser J, Kriz W. Synaptopodin: an actin-associated protein in telencephalic dendrites and renal podocytes. J Cell Biol. 1997;139(1):193-204.

44. Ling L, Chen L, Zhang C, Gui S, Zhao H, Li Z. High glucose induces podocyte epithelial-to-mesenchymal transition by demethylation-mediated enhancement of MMP9 expression. Mol Med Rep. 2018;17(4):5642-51.

45. Imasawa T, Obre E, Bellance N, Lavie J, Imasawa T, Rigothier C, et al. High glucose repatterns human podocyte energy metabolism during differentiation and diabetic nephropathy. FASEB J. 2017;31(1):294-307.

46. Wu M, Yang Z, Zhang C, Shi Y, Han W, Song S, et al. Inhibition of NLRP3 inflammasome ameliorates podocyte damage by suppressing lipid accumulation in diabetic nephropathy. Metabolism. 2021;118:154748.

47. Cao Y, Hu L, Chen R, Chen Y, Liu H, Wei J. Unfolded protein response-activated NLRP3 inflammasome contributes to pyroptotic and apoptotic podocyte injury in diabetic kidney disease via the CHOP-TXNIP axis. Cell Signal. 2025;130:111702.

48. Dandapani SV, Sugimoto H, Matthews BD, Kolb RJ, Sinha S, Gerszten RE, et al. Alpha-actinin-4 is required for normal podocyte adhesion. J Biol Chem. 2007;282(1):467-77.

49. Mosterd CM, Kanbay M, van den Born BJH, van Raalte DH, Rampanelli E. Intestinal microbiota and diabetic kidney diseases: the Role of microbiota and derived metabolites inmodulation of renal inflammation and disease progression. Best Pract Res Clin Endocrinol Metab. 2021;35(3):101484.

50. Alpers CE, Hudkins KL. Pathology identifies glomerular treatment targets in diabetic nephropathy. Kidney Res Clin Pract. 2018;37(2):106-11.

51. Barutta F, Bellini S, Gruden G. Mechanisms of podocyte injury and implications for diabetic nephropathy. Clin Sci (Lond). 2022;136(7):493-520.

52. Shankland SJ. The podocyte's response to injury: role in proteinuria and glomerulosclerosis. Kidney Int. 2006;69(12):2131-47.

53. Wang S, Li Y, Fan J, Zhang X, Luan J, Bian Q, et al. Interleukin-22 ameliorated renal injury and fibrosis in diabetic nephropathy through inhibition of NLRP3 inflammasome activation. Cell Death Dis. 2017;8(7):e2937.

54. Zhang C, Zhu X, Li L, Ma T, Shi M, Yang Y, et al. A small molecule inhibitor MCC950 ameliorates kidney injury in diabetic nephropathy by inhibiting NLRP3 inflammasome activation. Diabetes Metab Syndr Obes. 2019;12:1297-309.

55. Herman-Edelstein M, Thomas MC, Thallas-Bonke V, Saleem M, Cooper ME, Kantharidis P. Dedifferentiation of immortalized human podocytes in response to transforming growth factor-beta: a model for diabetic podocytopathy. Diabetes. 2011;60(6):1779-88.

56. Ning L, Suleiman HY, Miner JH. Synaptopodin deficiency exacerbates kidney disease in a mouse model of Alport syndrome. Am J Physiol Renal Physiol. 2021;321(1):F12-F25.

57. Honda K, Yamada T, Endo R, Ino Y, Gotoh M, Tsuda H, et al. Actinin-4, a novel actin-bundling protein associated with cell motility and cancer invasion. J Cell Biol. 1998;140(6):1383-93.

58. Di Donato A, Ghiggeri GM, Di Duca M, Jivotenko E, Acinni R, Campolo J, et al. Lysyl oxidase expression and collagen cross-linking during chronic adriamycin nephropathy. Nephron. 1997;76(2):192-200.

59. Komada T, Muruve DA. The role of inflammasomes in kidney disease. Nat Rev Nephrol. 2019;15(8):501-20.

60. Kume S, Koya D. Autophagy: A Novel Therapeutic Target for Diabetic Nephropathy. Diabetes Metab J. 2015;39(6):451-60.

61. Chawla A, Chawla R, Jaggi S. Microvasular and macrovascular complications in diabetes mellitus: Distinct or continuum? Indian J Endocrinol Metab. 2016;20(4):546-51.

62. Liu S, Yuan Y, Xue Y, Xing C, Zhang B. Podocyte Injury in Diabetic Kidney Disease: A Focus on Mitochondrial Dysfunction. Front Cell Dev Biol. 2022;10:832887.

63. Yang J, Savvatis K, Kang JS, Fan P, Zhong H, Schwartz K, et al. Targeting LOXL2 for cardiac interstitial fibrosis and heart failure treatment. Nat Commun. 2016;7:13710.

Abstract in Korean

당뇨병성 신증에서 Loxl2 억제가 염증복합체 발현에 미치는 영향

당뇨병성 신증(Diabetic nephropathy, DN)은 제1형 및 제2형 당뇨병 환자에게서 흔히 발생하는 미세혈관 합병증 중 하나로, 전 세계적으로 말기 신부전(End-stage renal disease, ESRD)의 가장 주된 원인 질환으로 알려져 있다. 당뇨병성 신증은 시간이 경과함에 따라 점진적인 사구체 여과율 감소와 지속적인 단백뇨, 신장 섬유화 및 기능 저하를 유발하며, 한 번 진행되기 시작하면 회복이 거의 불가능하다는 점에서 조기 병태기전의 규명과 표적치료 전략의 개발이 무엇보다도 중요하다. 사구체 내에서 여과 장벽을 구성하는 핵심 세포인 족세포(podocyte)는 기저막의 구조적 안정성을 유지하고, 단백질 여과를 조절하는 데 필수적인 역할을 수행하는 세포로, 당뇨병에 의한 대사 스트레스 및 면역 반응의 영향을 직접적으로 받는 취약한 세포군이다. 족세포 손상은 단백뇨의 직접적 원인일 뿐 아니라, 이후 발생하는 섬유화와 염증성 재구조화 과정의 주요 기전적 출발점이 되기 때문에 족세포 수준에서의 병인 규명은 DN의 근본적 이해를 위해 필수적이다.

최근 다양한 섬유화성 질환 및 종양 모델에서 Lysyl oxidase-like 2(Loxl2)는 세포외기질 성분의 교차결합 및 리모델링 과정에 중요한 역할을 하며, 염증 반응과 세포 내 신호전달 경로의 조절에 관여한다는 사실이 밝혀지고 있다. 특히, Loxl2는 TGF-β 경로를 포함한 섬유화 유도 사이토카인 신호의 상류 조절자로 기능하며, 조직 수준에서 구조적 변화와 염증성 환경을 동시에 유도하는 병리적 메커니즘의 중심에 존재할 가능성이 제기되고 있다. 그럼에도 불구하고, 당뇨병성 신증에서 Loxl2의 세포 특이적 발현 양상과 병태생리학적 기능, 그리고 염증성과 섬유화 간 연계된 병리 과정에서의 역할은 거의 연구되지 않았으며, 특히 족세포에 특이적으로 작용하는 메커니즘에 대한 분자 수준의 이해는 미흡한 실정이다.

이에 본 연구는 당뇨병 조건에서 족세포 내 Loxl2의 발현 변화를 확인하고, 해당 유전자가 질환의 진행 과정에 미치는 영향을 체계적으로 규명하고자 하였다. 이를 위해 인간 족세포 및 유전자 조작 마우스 모델을 기반으로 대사 스트레스 및 염증 자극에 대한 반응에서 Loxl2의 병태생리학적 역할을 규명하고, 염증 반응 및 세포외기질 리모델링과의 연관성을 분석하였다. 본 연구는 기존의 단순한 병변 억제 접근이 아닌, 세포 특이적 유전자 조절을 통해 질환의 근본적 병인 기전을 조절하려는 시도로서 의의가 있으며, 구조적 손상과 면역 반응이 복합적으로 얽혀 있는 당뇨병성 신증의 복잡한 병태기전에 대해 새로운 시각을 제시한다.

궁극적으로 본 연구는 Loxl2가 당뇨병성 신증에서 사구체 병변의 형성, 염증 유도성 면역 반응의 증폭, 그리고 섬유화 과정의 유지에 기여하는 주요 인자임을 제안하며, 족세포 특이적 Loxl2 억제 전략이 향후 질환의 진행을 지연시키거나 차단하는 데 효과적인 중재점이 될 수 있음을 보여주고자 한다. 또한 Loxl2를 표적으로 한 치료 전략은 기존 치료법들이 가지는 제한점들 예컨대 단백뇨의 부분적 개선이나 섬유화의 비가역성 등을 보완할 수 있는 새로운 접근으로서, 후속 약리학적 연구 및 임상 적용 가능성에 대한 기반자료를 제공한다. 더 나아가, 본 연구를 통해 규명된 Loxl2 중심의 병태 기전은 당뇨병성 신증뿐 아니라 다양한 만성 신장질환 및 대사성 질환의 치료 표적 탐색에도 확대 적용될 수 있는 학술적·임상적 가치를 지닌다.

핵심되는 말 : 당뇨병성 신증, 신장 질환, Loxl2, 족세포, Nlrp3, 염증복합체